

Probing and Knocking with Muons

Qiang Li

Qite Li, Chen Zhou

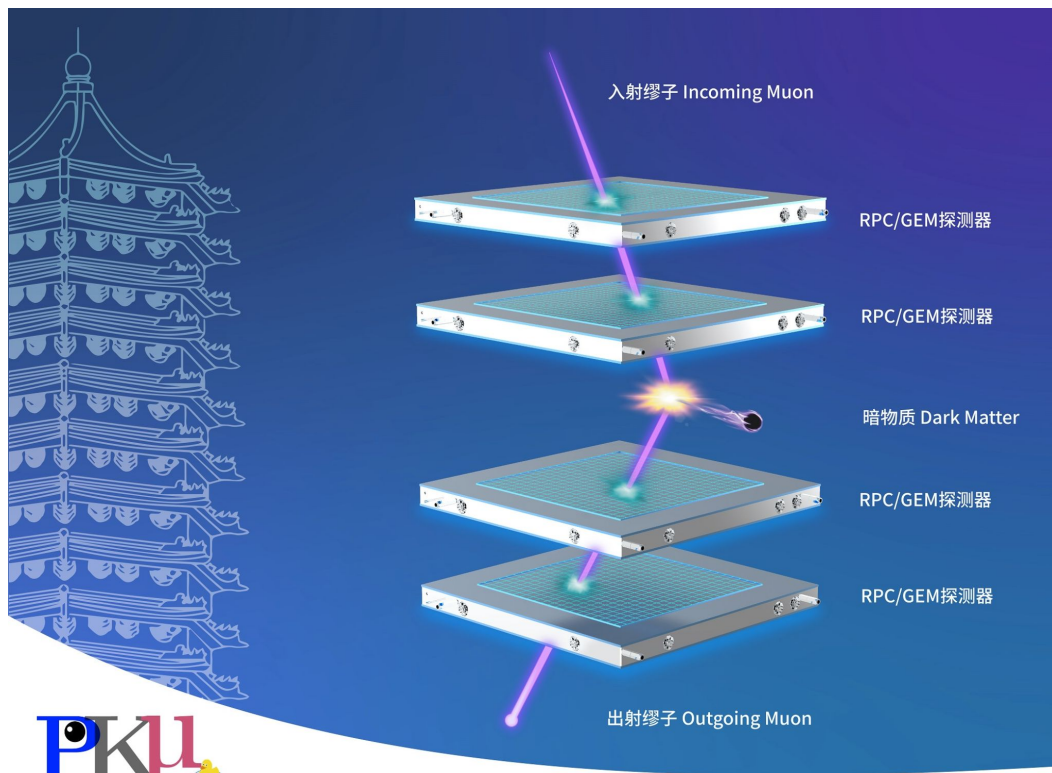
**On behalf of
the PKMu Group**

Peking University
2024 Fall

[Phys.Rev.D 110 \(2024\) 1, 016017](#)

[arXiv:2410.20323](#)

<https://lyazj.github.io/pkmuon-site/categories/activities/>



PKU Muon Detector Development



- CMS Muon Trigger RPC: assembled and tested at PKU at around 2002
- RPC R&D for nuclear physics
- CMS GEM upgrade program



北大基地生产的第一个CMS GEM模块



CMS端盖缪子探测器 GEM升级

北京大学、清华大学、中山大学、北京航空航天大学

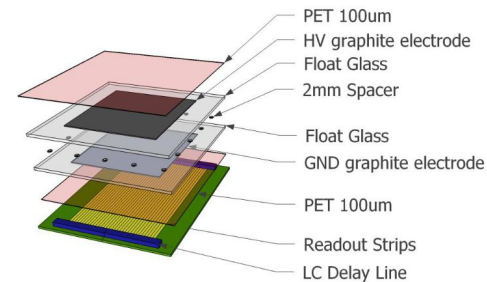
Combination of glass RPC & Delay-line Readout



Study of spatial resolution properties of a glass RPC
 Qi-te Li, Yanlin Ye*, Chao Wen, Wei Ji, Yushou Song, Rongrong Ma, Chen Zhou, Yucheng Ge, Hongtao Liu
 School of Physics and State Key Laboratory of Nuclear Physics and Technology, Peking University, Beijing 100871, China

Reference:

- 许金艳, 李奇特*, 等, *物理实验*, 41(2021)23
- Qi-Te, Li, et al. *Chinese Physics C* 37 (2013)016002.
- S. Chen, Q. Li*, et al, *JINST*: 10 (2014)10022.

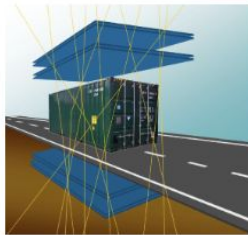


90% R134a+9% i-C4H10+1% SF6 50ml/Min

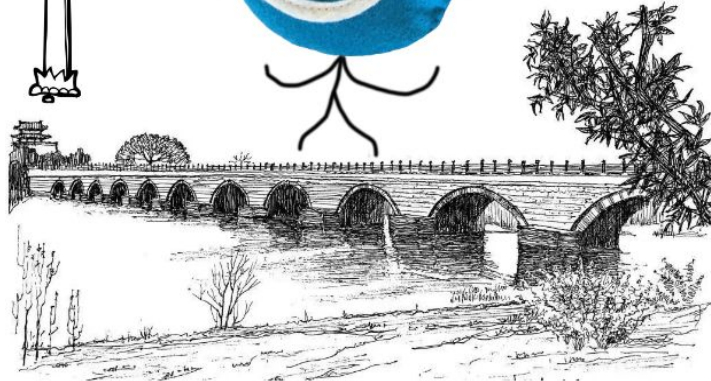
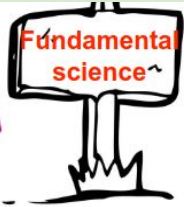
Muon: a bridge connecting applied and fundamental particle physics



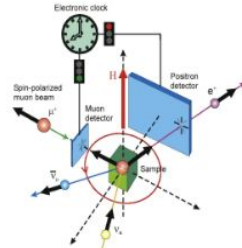
Void in Pyramid



Container inspection

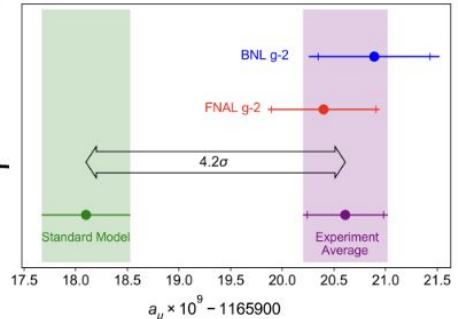


Bridge in Beijing



muSR

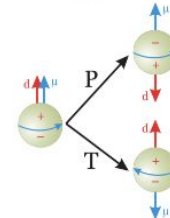
- Heavy fermion
- Superconductivity
- Quantum spin liquid
- ...



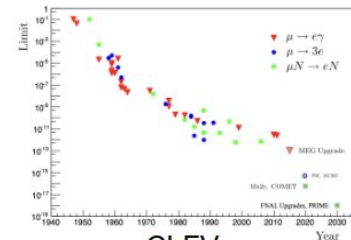
Muon g-2

Fundamental particle physics

- Muon g-2
- Muon EDM (Electric Dipole Moment)
- Muon CLFV (Charged Lepton Flavor Violation)
- Muon-philic DM (NA64 μ , MMM, this work)
- ...



EDM



CLFV

Muongraphy: Non-destructive property!

- Geology:
 - Rock formations, glaciers, minerals, oceans and underground carbon dioxide storage*
- Archaeology:
 - pyramids in Egypt, Mausoleum of Qin Shihunag*
- Volcano monitor:
 - Showa-Shinzan, Asama, Sakurajima in Japan, and Stromboli in Italy*
- Tropic Cyclones monitor:
 - Kagoshima, Japan*
- Nuclear safety monitor:
 - Visualization of reactor interiors, detection of spent nuclear fuel in dry storage barrels and nuclear waste*
- ...

Workshop on Muon Physics at the Intensity and Precision Frontiers (MIP 2024)

19 Apr 2024, 02:00 → 22 Apr 2024, 12:20 Asia/Shanghai

Peking University

Chen Zhou (Peking University (CN)), Qiang Li (Peking University (CN)), Qite Li (Peking University)



MIP2024

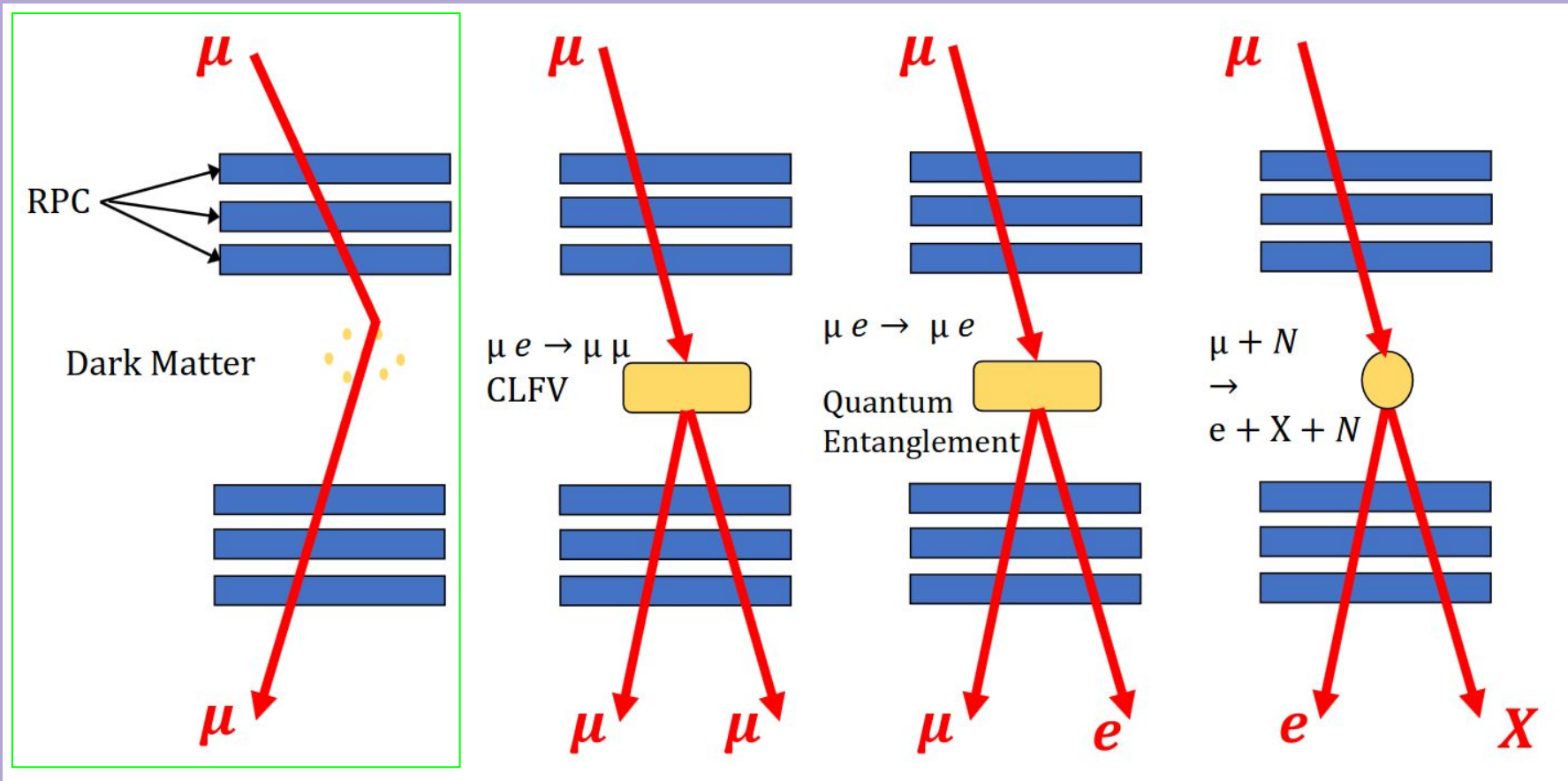
Several possible
Chinese Muon beams
in the near future:
Melody,
CIADS, HIAF

缪子散射类型的实验在国际上较为欠缺。 Large potential on muon scattering exp. (Pre/Mid-CEPC; Quantum Physics; Muon Scattering)

一方面, 1960年代欧美的一些实验(例如[Phys. Rev. 137, B266, 1965](#))等侧重于探测核性质。由于当时标准模型尚未完整建立, 对利用缪子进行带电轻子味道破坏、暗物质等新物理的寻找还不成熟; 另一方面, 在近几个世纪, 利用缪子对新物理的探索, 例如美国的缪子反常磁矩实验、欧洲的缪子反常衰变的探测如MEG、Mu3e等实验, 通常采用的是自由缪子或缪子衰变。直到近年来, CERN的NA64mu([Phys. Rev. Lett. 132, 211803](#))和设计中的MuonE等实验才开始重新利用高能缪子($\sim 160\text{GeV}$)与靶散射, 通过对缪子与核子或电子的散射来对新物理或者重要的标准模型观测量进行探索。

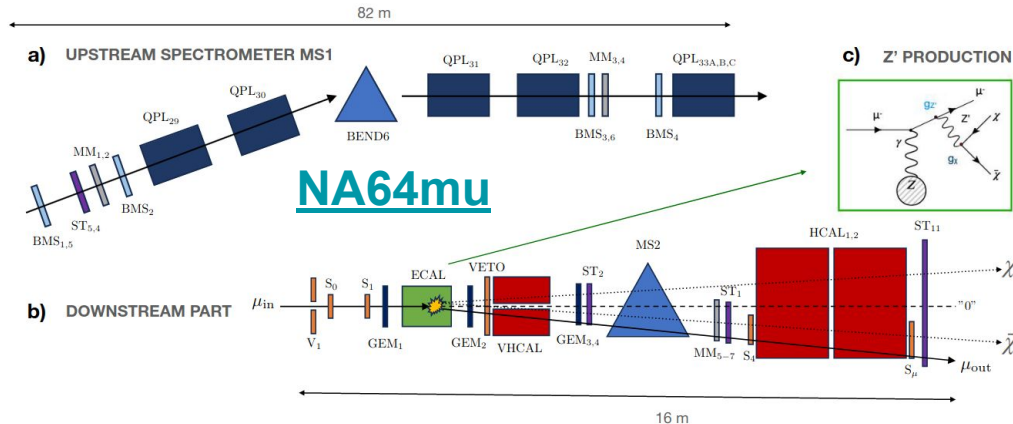
然而, **缪子散射蕴含大量的物理课题有待挖掘, 而且不同能量的缪子束流可以对不同的新物理空间具有敏感性**。如下所述, 缪子与可能的亲缪子类型暗物质可以发生大角度散射; 缪子与电子的散射可以用来探测带电轻子味道破坏的新型玻色子; 对GeV缪子与电子散射的精确测量也可以来验证量子纠缠([Phys. Rev. D 107, 116007 \(2023\)](#)); 缪子与核子的散射则可以探测不同核子的性质, 由于质心系能量相比缪子与静止电子的高, 也可以探测更高能标的不同种类的新物理。

Probing and Knocking with Muons



Muon Philic Dark matter

- Muon Philic Dark Matter may be possible or necessary!
- Electron/Muons on Target Experiments
- DarkShine is ~ LDMX based on Shanghai Synchrotron Radiation Facility
- MMM (M3) is a US proposed muon-LDMX experiment
 - Intrigued by a proposal based on CERN NA64
 - “a lower-energy, e.g. 15 GeV, muon beam allows for greater muon track curvature and, therefore, a more compact experimental design...”



Light Dark Matter

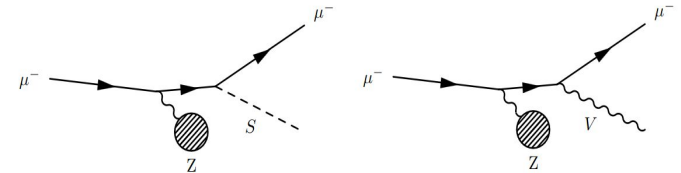


Figure 1. Dark bremsstrahlung signal process for simplified models with invisibly decaying scalar (left) and vector (right) forces that couple predominantly to muons. In both cases, a relativistic muon beam is incident on a fixed target and scatters coherently off a nucleus to produce the new particle as initial- or final-state radiation.

Exotic Dark Matter concentrated near the Earth

PHYSICAL REVIEW LETTERS 131, 011005 (2023)

Dark Matter Annihilation inside Large-Volume Neutrino Detectors

Owing to their interactions with ordinary matter, a strongly interacting dark matter component (DMC) would be trapped readily in the Earth and thermalize with the surrounding matter. Furthermore, for lighter DM, strong matter interactions allow Earth-bound DM particles to distribute more uniformly over the entire volume of the Earth rather than concentrating near the center. Together, this can make the DM density near the surface of the Earth tantalizingly large, up to $\sim f_\chi \times 10^{15} \text{ cm}^{-3}$ for DM mass of 1 GeV [8–11]. Despite their large surface abundance, such thermalized DMCs are almost impossible to detect in traditional direct detection experiments as they carry a minuscule amount of kinetic energy $\sim kT = 0.03 \text{ eV}$. A

- A large amount of dark matter is concentrated near the Earth, and their speed is very low, making it difficult to cause recoil signals in experiments. (大量暗物质集中在地球附近, 它们的速度很低, 很难在实验中引起足够的反冲信号)
- **As we will see, muon DM scattering experiment (PKMuon) depends minorly on DM velocity**

Muon Tomography and Muon-DM scattering

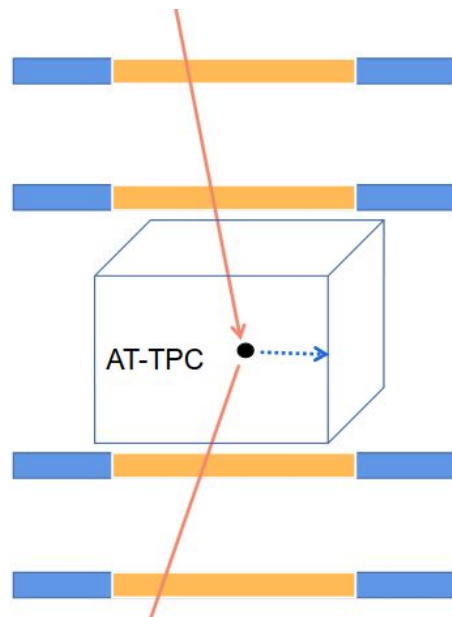
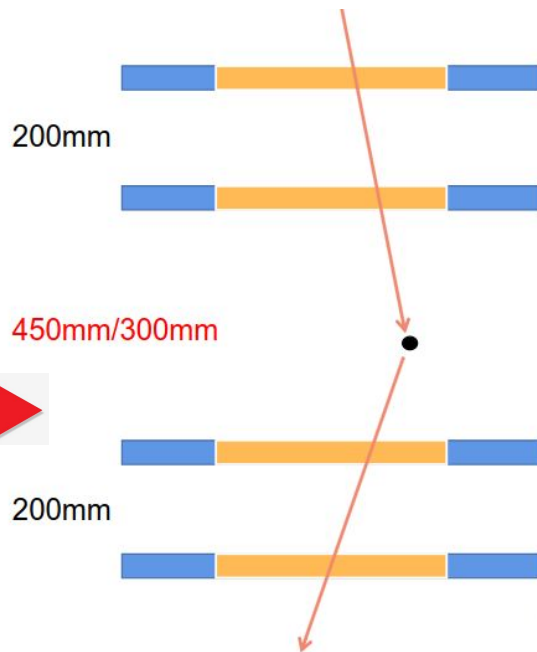
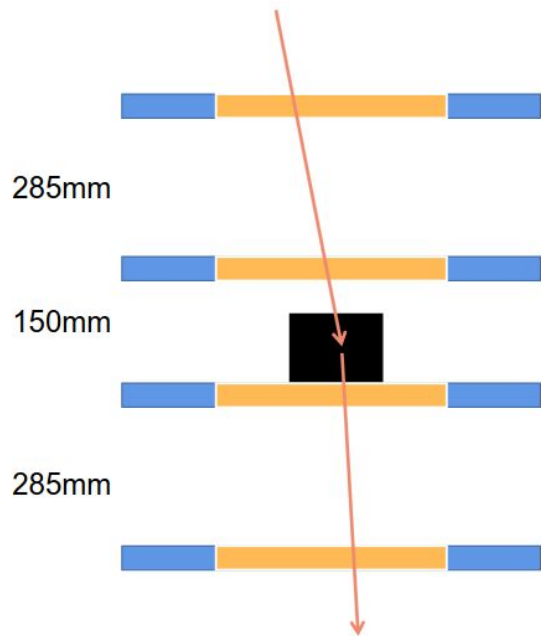
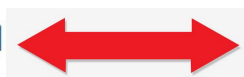
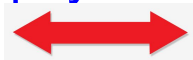
Muon Tomography

繆子成像

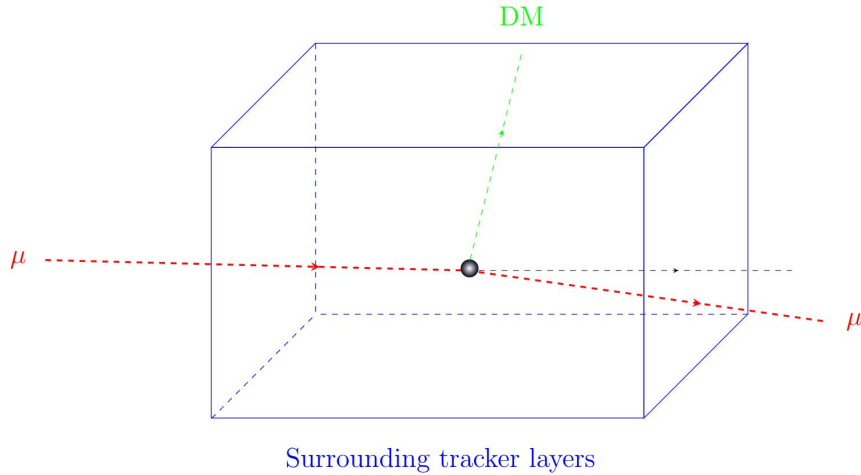
Dark Matter Search

暗物质寻找

[Phys.Rev.D 110 \(2024\) 1, 016017](#)



Muon DM Box experiment: qualitative estimation



Notice for high speed muons, it is appropriate to treat DM as frozen in the detector volume (V), and the estimated rate per second could be:

$$\rho V / M_D \times \sigma_D \times F_\mu,$$

The local density of DM is at the order of $\rho \sim 0.3$ GeV/cm³ and with a typical velocity of $v = 300$ km/s. While F_μ is the muon flux $\sim 1/60$ /s/cm² at the sea level. For Dark Matter mass $M_D \sim 0.1$ GeV, and detector box volume as $V \sim 1$ m³. Thus the sensitivity on Dark Matter Muon scattering cross section for 1 year run will be around

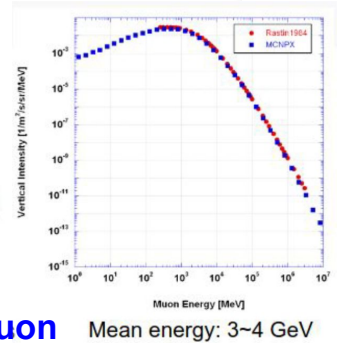
$$\sigma_D \sim 10^{-12} \text{ cm}^2 \quad \text{One year}$$

In the exotic DM scenario as mentioned previously, the limit can approach μb

Muon DM Box experiment: Geant4 Simulation

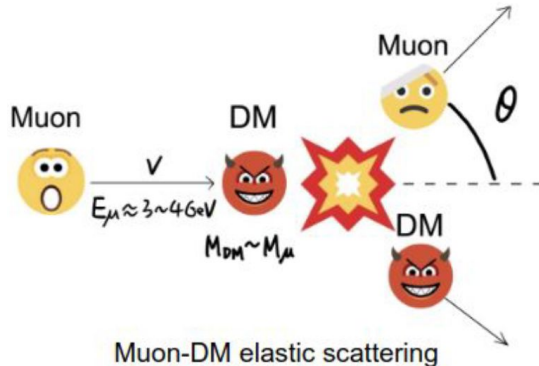
→ MC simulation of GEM-based detector based on **Geant4**

- ❖ Triple-GEM detector design refer to [CMS GEM design](#)
- ❖ Muon material interaction automatically considered by Geant4
- ❖ Reco hit position: Truth hit position smeared by GEM detector resolution (~ 200 um)



→ DM and muon scattering: **model-independent method**

- ❖ Non-relativistic two-body elastic scattering between muon and DM following Newtonian mechanics
- ❖ Standard halo model: DM velocity distribution follows Maxwell-Boltzmann distribution
- ❖ [CRY](#) (Cosmic-ray) model: cosmic-ray muon energy and zenith angle distributions at sea-level



**Different from XENON1T/PandaX:
Relativistic muon hit quasi-static DM**

Muon DM Box experiment: Geant4 Simulation

Cos θ distribution in air has no obvious difference between that in a vacuum. Considering cost and technical difficulty, **vacuuming of the boxes is not necessary in Phase I of the project.**

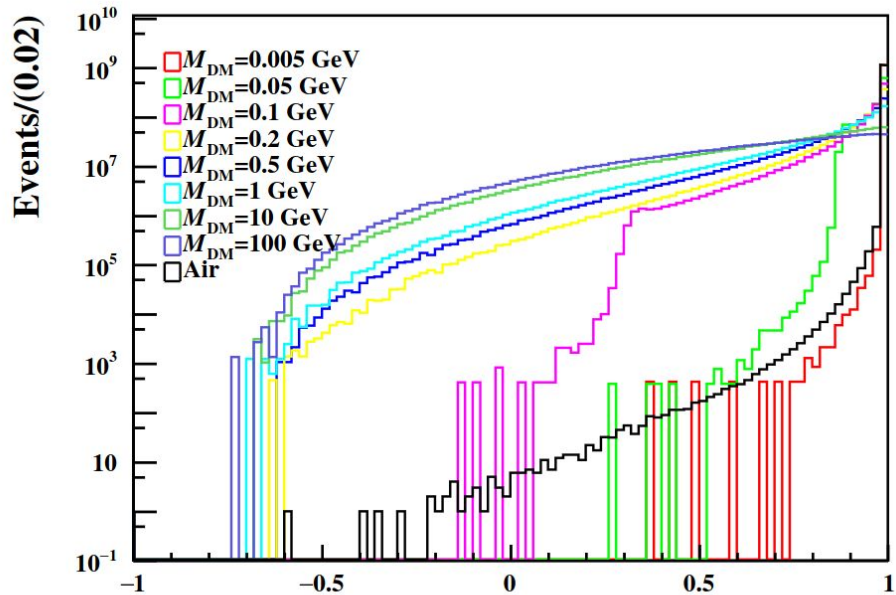
Cos θ distributions in Maxwell-Boltzmann velocity distribution and a constant velocity distribution are similar. Therefore, **our signal distribution and detection is not sensitive to the DM velocity model.**

As the DM mass increases, a larger fraction occupies the region of large scattering angles, resulting a more pronounced discrepancy between the signal and background.

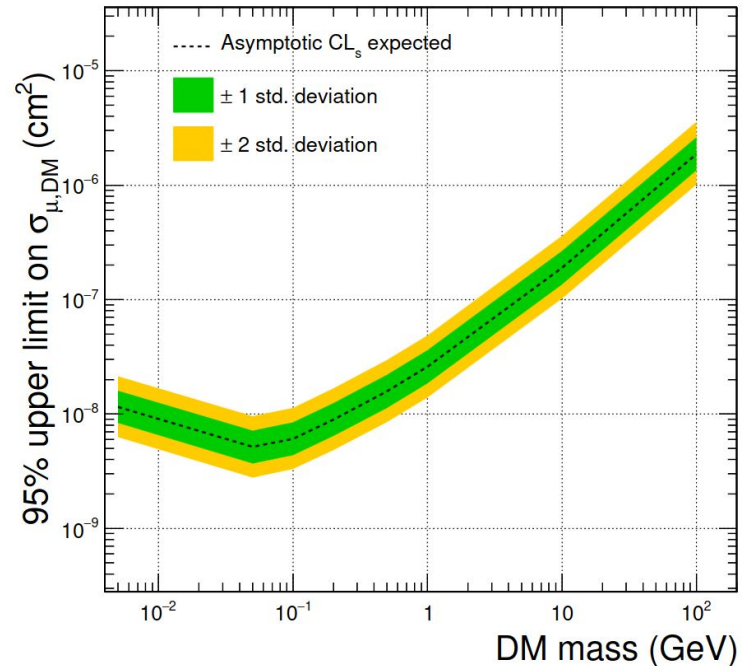
Background	Event Number ($\times 10^9$)	
Air	1.15	
Vacuum	1.14	
DM mass (GeV)	Constant (%)	Maxwell-Boltzmann (%)
0.005	27.10 ± 0.01	27.11 ± 0.01
0.05	29.56 ± 0.01	29.55 ± 0.01
0.1	27.66 ± 0.01	27.64 ± 0.01
0.2	25.01 ± 0.01	24.99 ± 0.01
0.5	21.47 ± 0.01	21.46 ± 0.01
1	18.67 ± 0.01	18.66 ± 0.01
10	11.10 ± 0.01	11.10 ± 0.01
100	8.44 ± 0.01	8.43 ± 0.01

TABLE I. Background event numbers corresponding to the integrated luminosity of one-year exposure with the box filled with air and vacuum, along with the signal detection efficiency under different assumptions of DM velocity distribution and mass.

Muon DM Box experiment: expected results

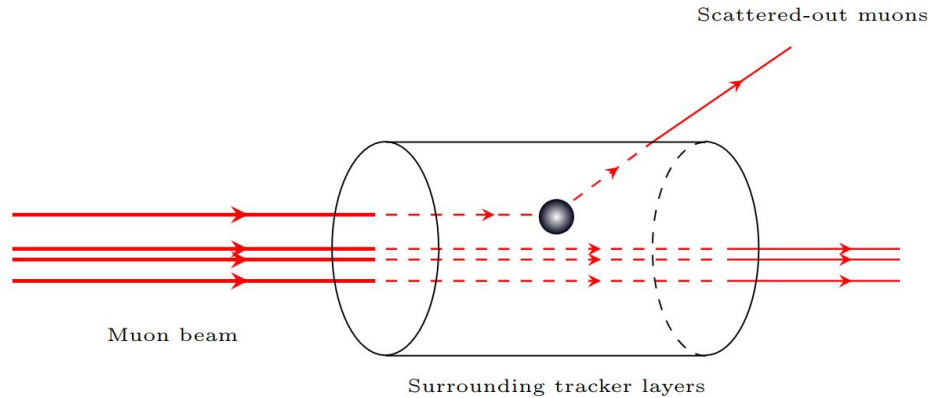


- “Asimov” data is used
- Binned maximum likelihood fits
- UL determined by CLs method
- Only take statistical uncertainty into consideration



In the exotic DM scenario as mentioned previously, the limit can approach μb

Muon DM Beam experiment: qualitative estimation



For $M_D = 0.03 \text{ GeV}$, $L = 1 \text{ m}$, and $N_\mu \sim 10^6/\text{s}$ (e.g., CSNS Melody design), and one year 10^7 s .

$$N = 10^{13} \times \sigma_D \times 100/\text{cm}^2,$$

Thus the sensitivity on Dark Matter Muon scattering cross section for 1 year run will be around

The estimated rate per second:

$$dN/dt = N_\mu \times \sigma_D \times L \times \rho/M_D,$$

$$\sigma_D \sim 10^{-15} \text{ cm}^2$$

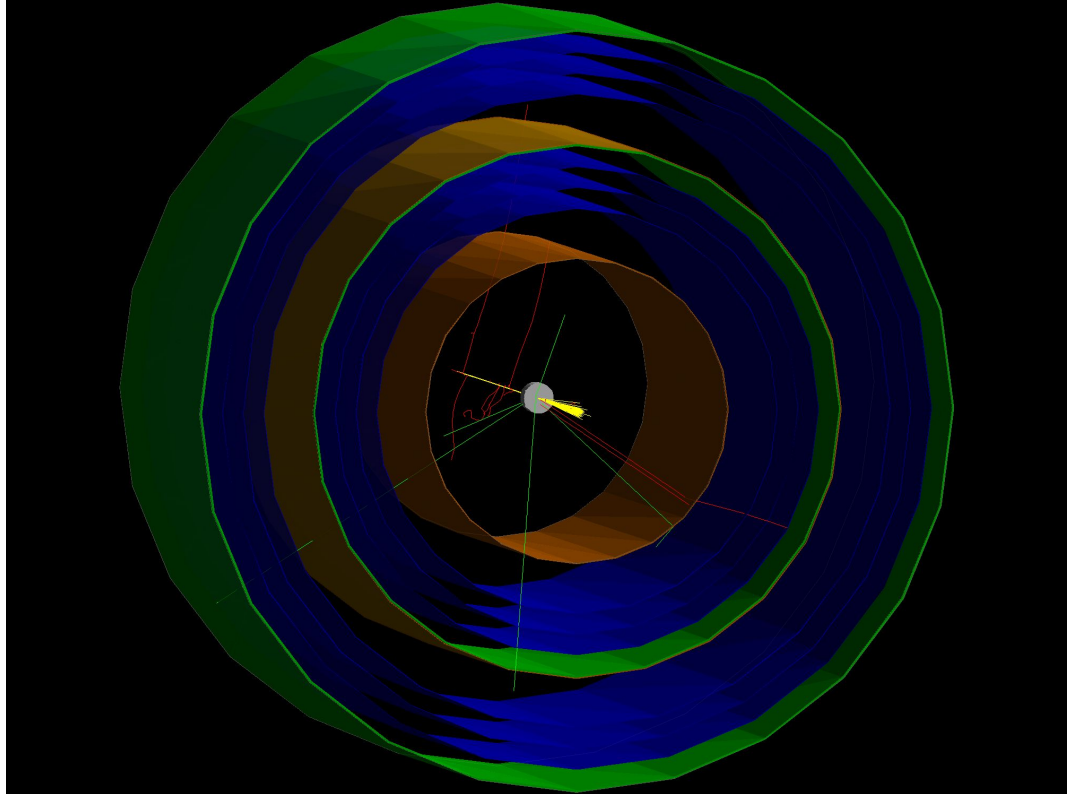
One year

Notice the surrounding area can be as small as 100 cm^2 .

Muon DM Beam experiment: Geant4 Simulation

Simulating 1 GeV muon beam hit lead plate passing through GEM detector: the inner diameter of our CGEM detector is designed to be **50 mm**, which is **5 times the beam spot**.

Orange surfaces are drift cathodes. The blue surfaces are GEM foils. The green surfaces are PCBs. The yellow lines are muons tracks. The red curves are electron tracks. The green lines are photons.



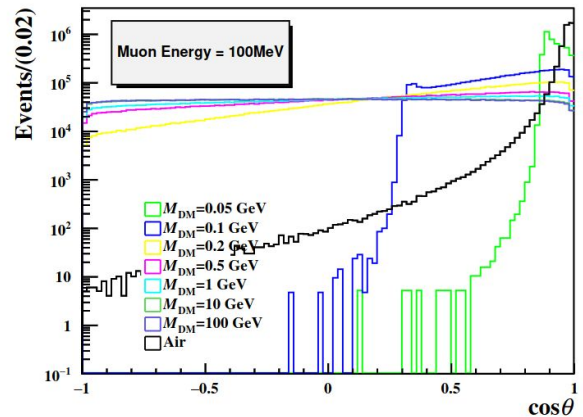
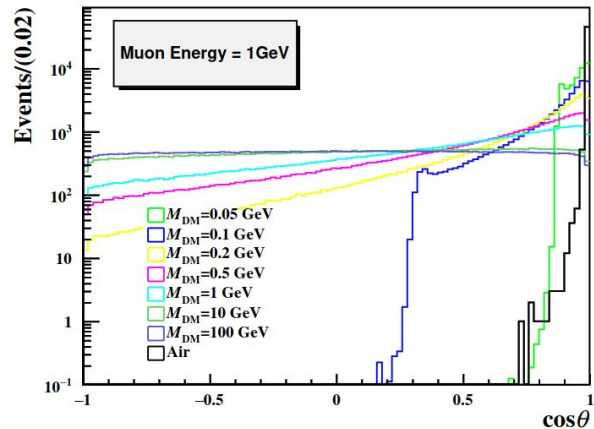
Cylindrical GEM (CGEM) detector structure for BESIII inner tracker system upgrade

Muon DM Beam experiment: Geant4 Simulation

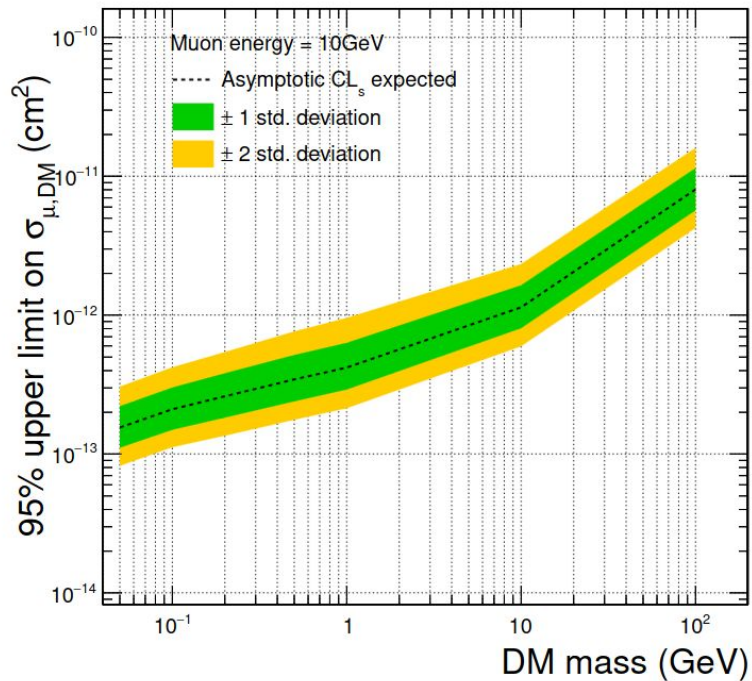
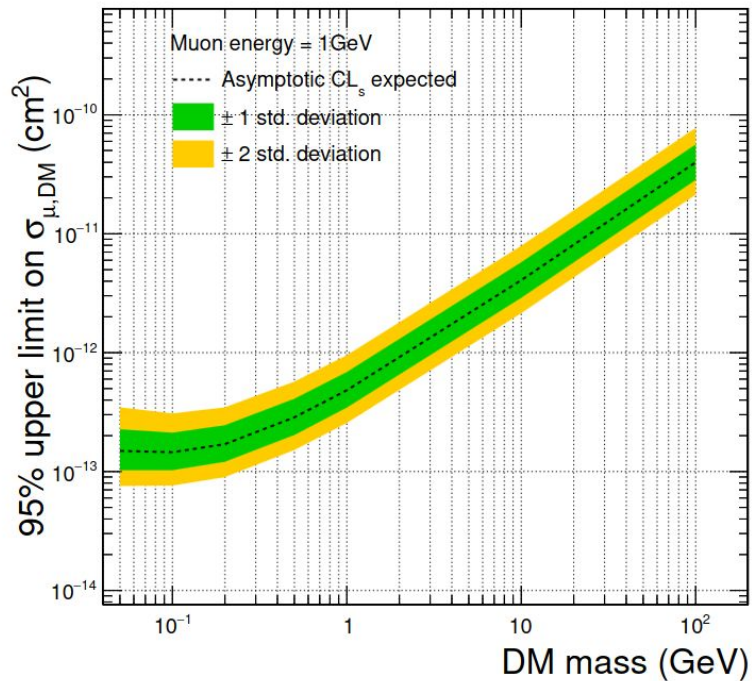
If the scattering angle is large enough, muons may hit the surrounding detector.

$M_{\text{DM}} \setminus E_{\text{kin}}^\mu$	100 MeV (%)	1 GeV (%)	10 GeV (%)
0.05 GeV	84.29 ± 0.04	74.85 ± 0.04	45.93 ± 0.05
0.1 GeV	91.74 ± 0.03	83.07 ± 0.04	58.17 ± 0.05
0.2 GeV	94.35 ± 0.02	88.16 ± 0.03	68.37 ± 0.05
0.5 GeV	95.17 ± 0.02	92.16 ± 0.03	78.91 ± 0.04
1 GeV	95.34 ± 0.02	93.88 ± 0.02	84.68 ± 0.04
10 GeV	95.35 ± 0.02	95.36 ± 0.02	94.06 ± 0.02
100 GeV	95.43 ± 0.02	95.37 ± 0.02	95.37 ± 0.02

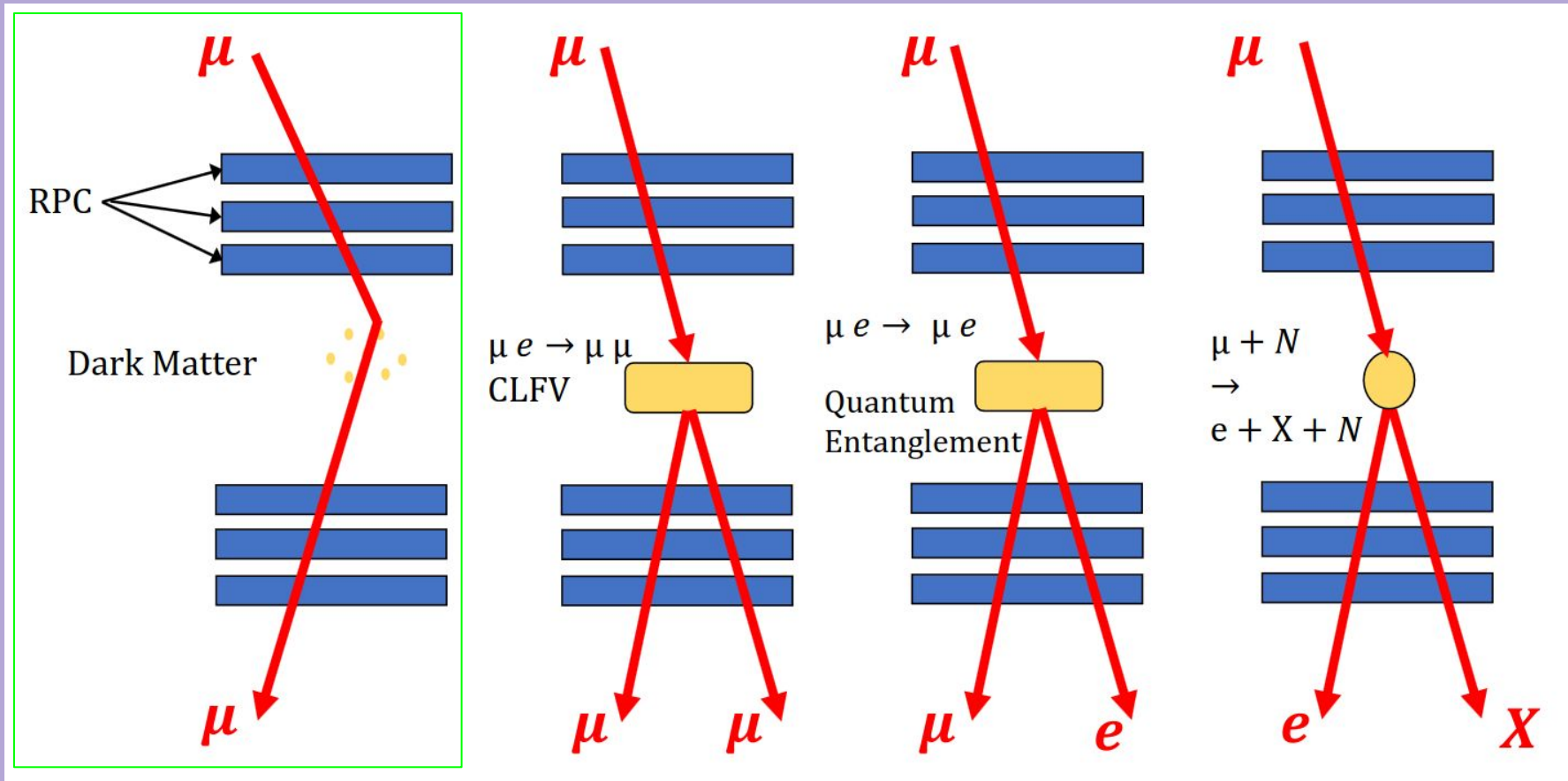
TABLE II. Signal detection efficiency under different assumptions of DM mass and muon beam energies.



Muon DM Beam experiment: Geant4 Simulation



Probing and Knocking with Muons



Current Software and Simulation Status



PKMuon Collaboration

PKMuon Collaboration

3 followers China <https://lyazj.github.io/pkmuon-site/> seeson@pku.edu.cn

[Overview](#) [Repositories](#) 10 [Projects](#) [Packages](#) [People](#) 2

Pinned

[PKMUON_G4sim](#) Public

Forked from yuxdPKU/PKMUON_G4sim

Geant4-based simulation of PKMUON

● C++

[geomu](#) Public

Forked from lyazj/geomu

Geographic Muon Simulation

● C++

[pkmuon-site-src](#) Public

Forked from lyazj/pkmuon-site-src

source code of PKMUON site

● Stylus

[root-easy-debug](#) Public

Forked from lyazj/root-easy-debug

Debug CERN ROOT macros in an extremely easy way

● C

PHYSICAL REVIEW D **110**, 016017 (2024)

Proposed Peking University muon experiment for muon tomography and dark matter search

Xudong Yu,^{*} Zijian Wang, Cheng-en Liu, Yiqing Feng[✉], Jinning Li, Xinyue Geng, Yimeng Zhang, Leyun Gao, Ruobing Jiang, Youpeng Wu, Chen Zhou^{✉,†}, Qite Li^{✉,‡}, Siguang Wang, Yong Ban[✉], Yajun Mao, and Qiang Li^{✉§}

State Key Laboratory of Nuclear Physics and Technology, School of Physics, Peking University, Beijing, 100871, China

(Received 23 March 2024; accepted 24 June 2024; published 19 July 2024)

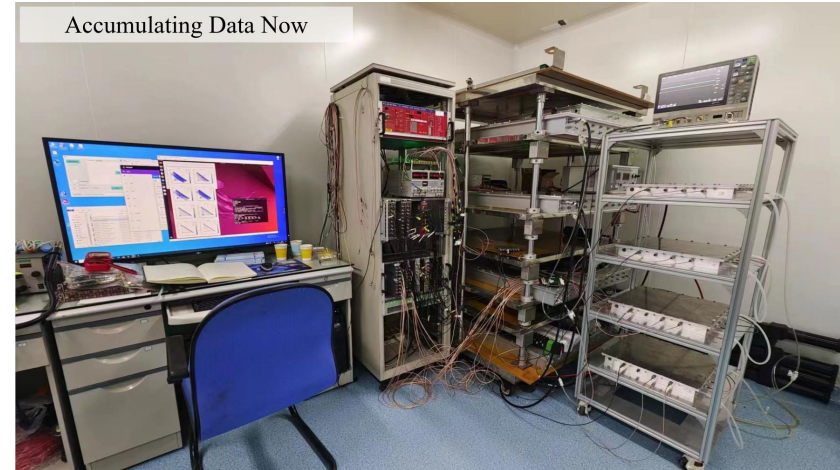
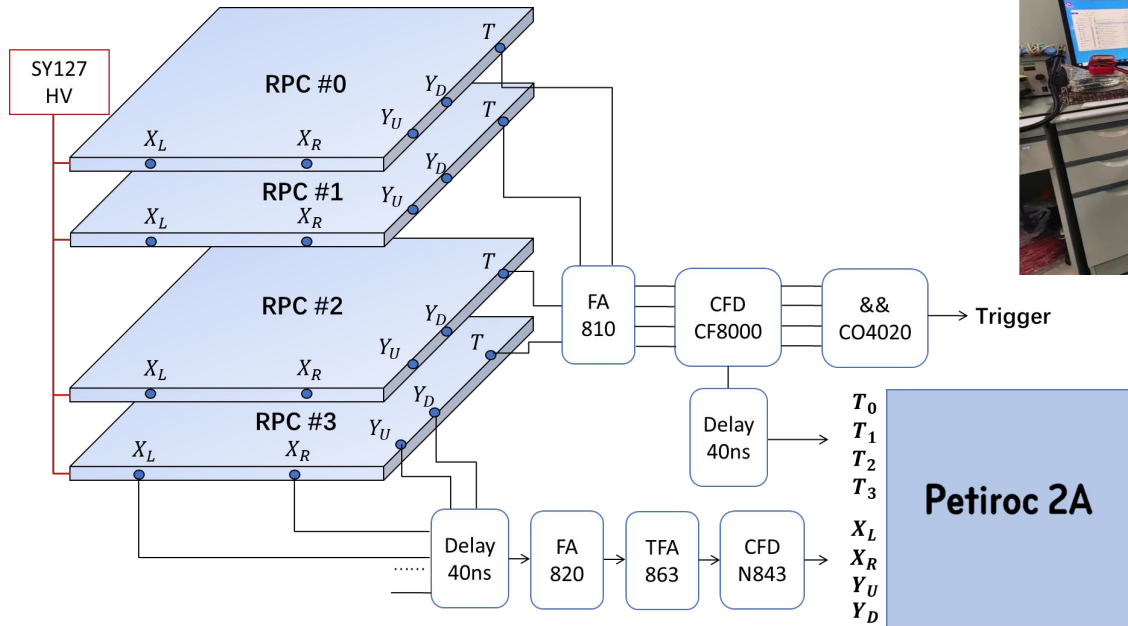
A set of new methods are proposed here to directly detect light mass dark matter through its scattering with abundant atmospheric muons or accelerator beams. A first plan is to use the free cosmic-ray muons interacting with dark matter in a volume surrounded by tracking detectors, to trace the possible interaction between dark matter and muons. Secondly, the same device can be interfaced with domestic or international muon beams. Due to the much larger muon intensity and focused beam, it is anticipated that the detector can be made further compact, and the resulting sensitivity on dark matter searches will be improved. Furthermore, it may also be possible to measure precisely directional distributions of cosmic-ray muons, either at mountain or sea level, and the differences may reveal possible information about dark matter distributed near the Earth. Specifically, methods described here can have advantages over “exotic” dark matters that are either muonphilic or slowed down due to some mechanism, and the sensitivity on dark matter and muon scattering cross section can reach as low as microbarn level.

DOI: 10.1103/PhysRevD.110.016017

Current Box Exp. Status

4-station 20cm*20cm RPC for the moment

Petiroc 2A is a 32-channel front-end ASIC

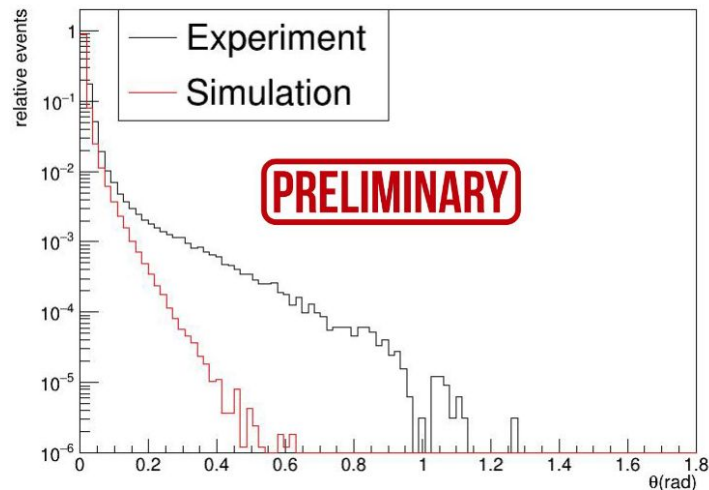
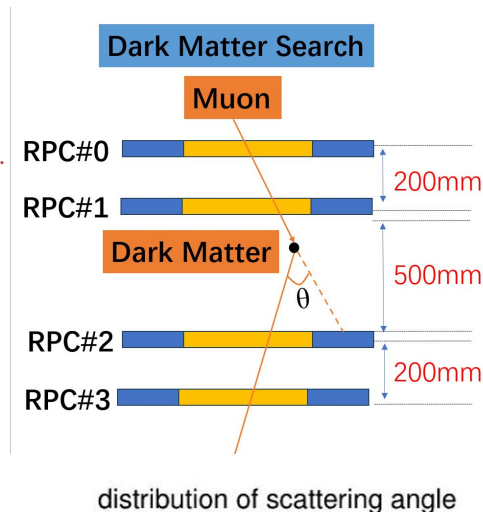


Timing and X-Y position
with delay-line readout
method

Accumulated Data

- 3+ months data taking since Jan. 2024
- Effective volume as $50\text{cm} \times 20\text{cm} \times 20\text{cm}$
- Total effective events as 330548, with mean scattering angle as 0.0252 rad
- The fraction of large angle scatter events ($\theta > 0.2 \text{ rad}$) is around 1.6%
- There are several events with $\cos \theta < 0.4$
- Data Analysis is ongoing

More results in [a recent report](#) from Cheng-en Liu and Qite Li



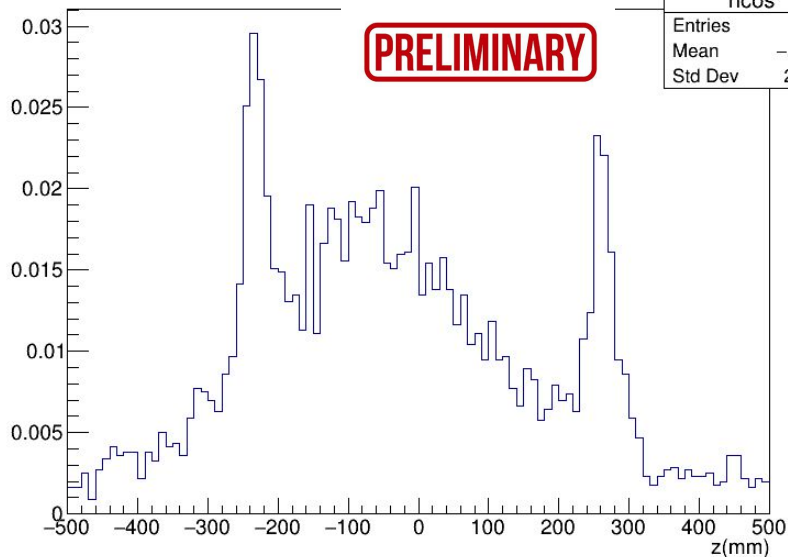
Large angle events

Many around RPC locations

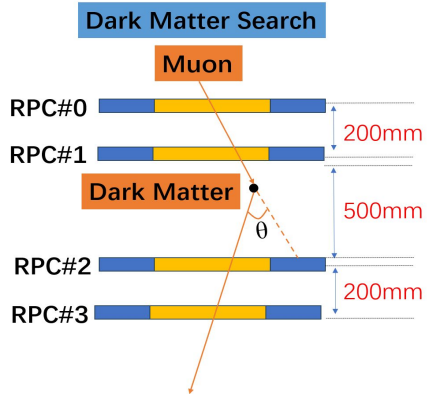
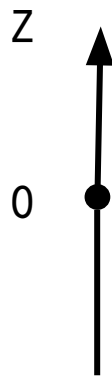
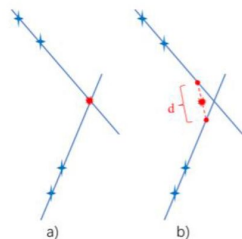
Z Events($\theta > 0.2$ rad)

PRELIMINARY

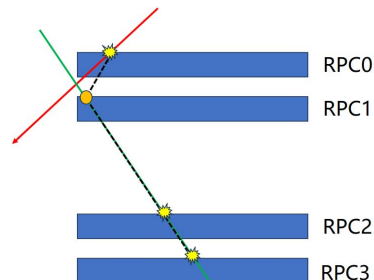
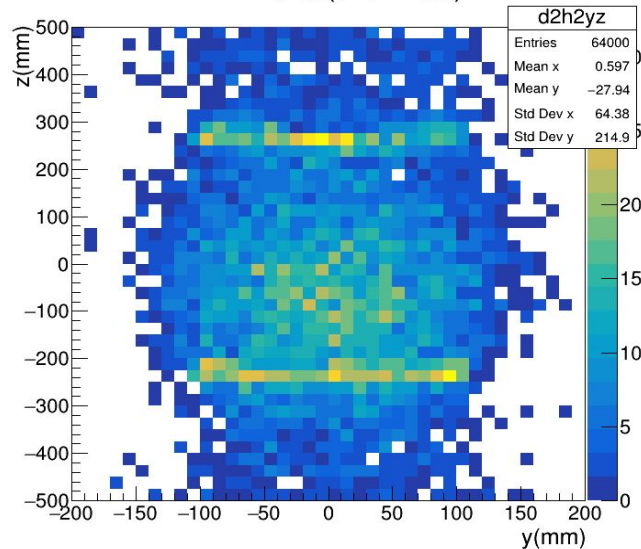
hcos	
Entries	5578
Mean	-29.81
Std Dev	210.3



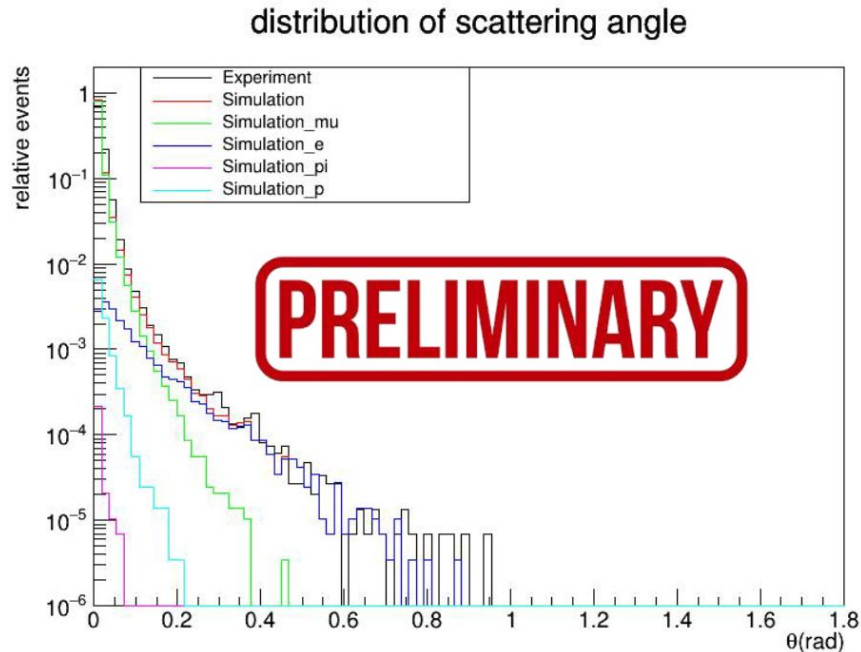
Distance between skew lines



YZ Events($\theta > 0.2$ rad)



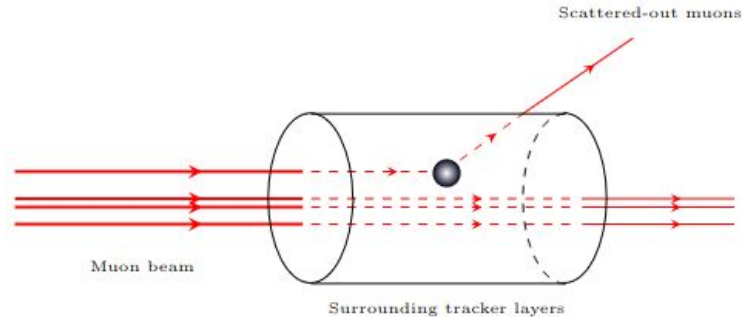
- 有效事件147251, $\theta > 0.2\text{rad}$ 事件占比0.37%
- 平均散射角0.0193rad
- 对海平面上次级宇宙线粒子成分进行模拟: μ , e, pi, p
- 小角度主要为缪子, 大角度主要为高能电子(物理过程检查中)
- 部分理解了大角度散射的来源
- 为改善缪子探寻暗物质的探测下限, 需进行对高能电子的本底事件排除



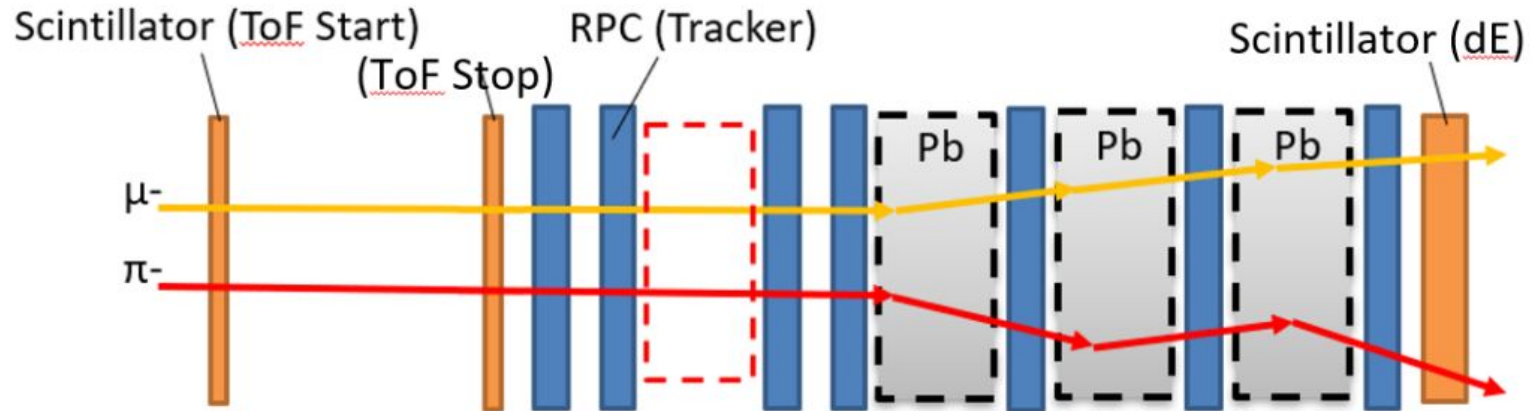
**Stay
Tuned!**

Current Beam Exp. Status

Interfacing with a muon beam at e.g. HIAF



Cylindrical GEM (CGEM)
detector structure for BESIII
inner tracker system upgrade



Current Beam Exp. Status

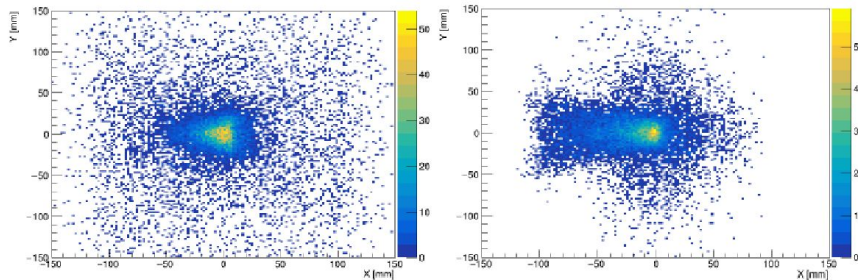


图 6.9: 左: 1GeV 缪子束流束斑轮廓。右: 3GeV 的缪子束流的束斑轮廓

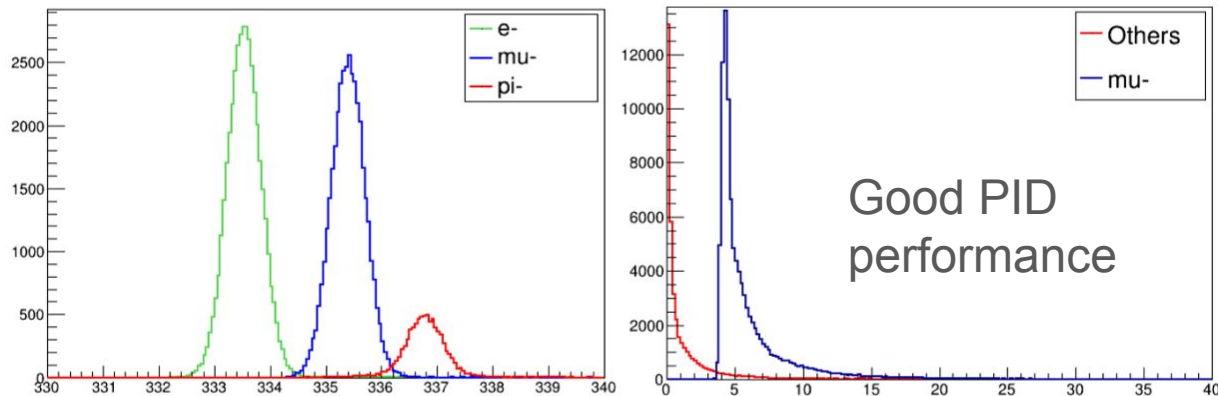


图 6.13: 缪子散射探测系统信号与背景响应模拟: 成像系统前飞行时间谱 (左); 末端闪烁体能量损失谱 (右)

惠州大科学装置高精度物理实验调研报告

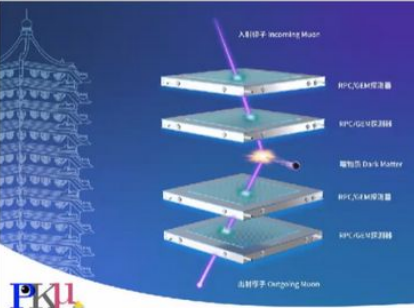
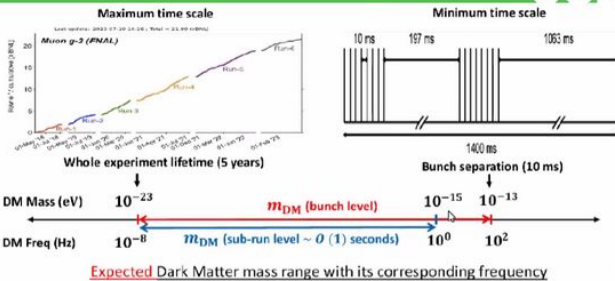
Research report on high-precision physics experiments at Huizhou Big Science Facility

To appear soon

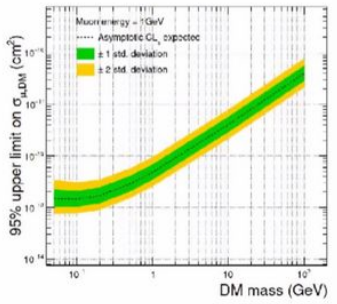
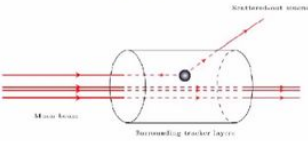
NuFact 2024 is the 25th in the series of yearly international workshops which started in 1999 and which had previously been called the International Workshop on Neutrino Factories.

Byungchul Yu
Scalar DM search with Muon g-2:
- induce oscillation in muon mass at DM freq.

$$\omega_a(t) = a_\mu \frac{q}{m(t)} B$$



Qiang Li
Muon - DM scattering
- tomography, or muon beam



Goodman, Maury C. 17 Oct 2024, 03:02

American experimental particle physicist at the [Argonne National Laboratory](#). He earned his undergraduate degree at the [Massachusetts Institute of Technology](#) (1972) and his PhD (1979) at the [University of Illinois, Urbana-Champaign](#) under the supervision of [Albert Wattenberg](#).

APS fellow 2008, served for seven years as Leader of the ANL-HEP Neutrino Group. He has been Deputy Spokesperson of the LBNE collaboration (2010 to present).

Dear Qiang,

Review of Nufact2024-01

C. Zhou, Q. Li and Q. Li for the PKMu collaboration,
“Probing and Knocking with Muons for Dark Matter and others”



This is an interesting paper. It presents an idea with which I wasn't familiar; i.e. looking for large angle muon scattering as an indication of Dark Matter-muon interactions...

I would be surprised if this was the first suggestion of using large angle muon scattering to constrain Dark Matter. But it may be the case.

Several previous large detectors which measure muons would be sensitive to this, but may not have calculated limits.

05:10:04



Thank you all for your participation!

We have had 58 talks

- New detectors
- New techniques
- Great progress on applying Machine learning to MT
- Artificial muon sources
- Even using MT to look for dark matter

Next workshop

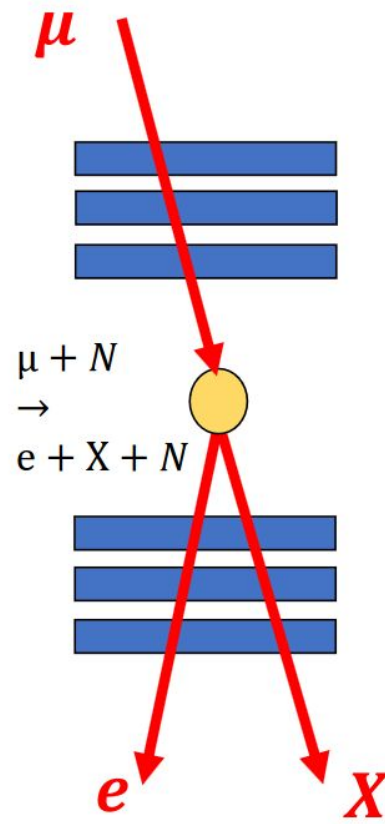
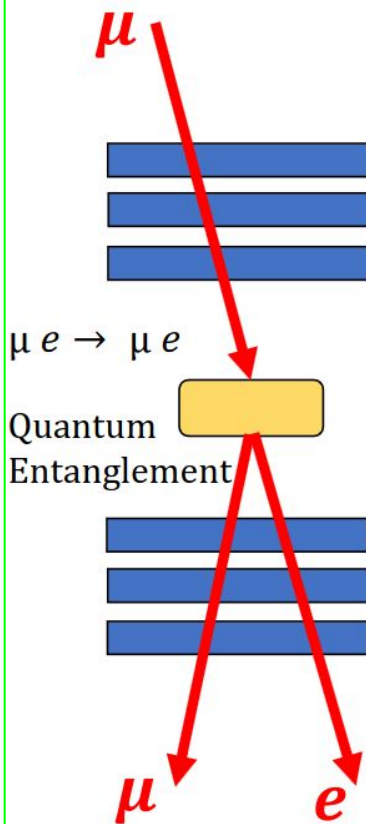
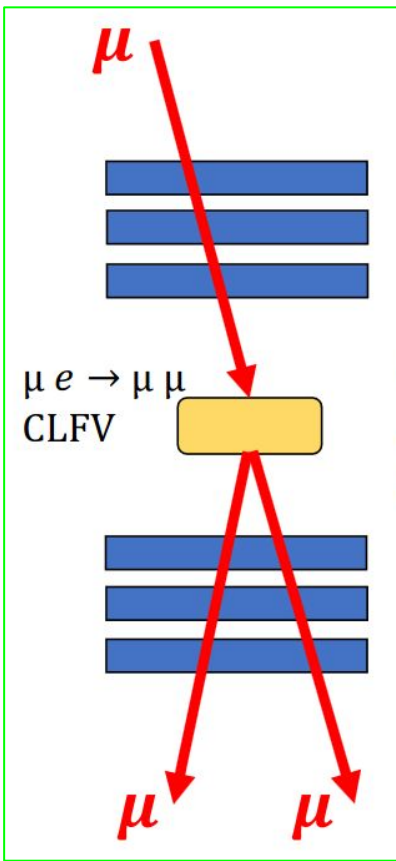
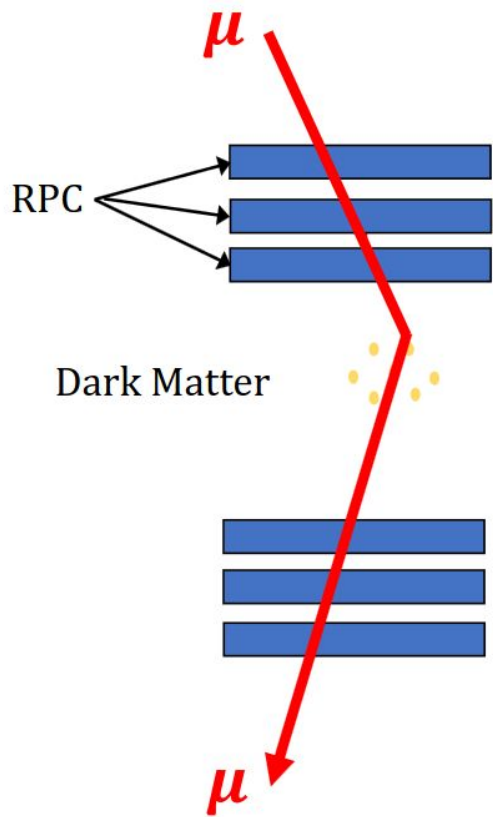
- Michael Tygat is requesting input michael.tygtat@cern.ch
discussion at lunch
- Let's hope for exciting weather!

The organizers will work (with permission) to make talks
on the web in the next few weeks

Missy Barlow (1/20)

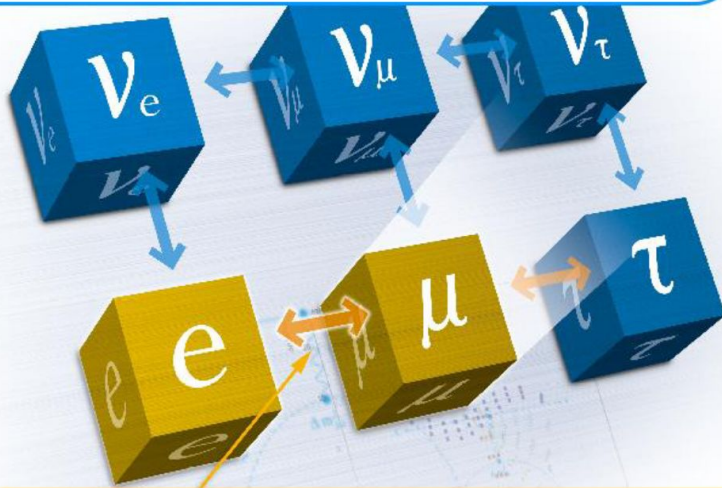


Probing and Knocking with Muons



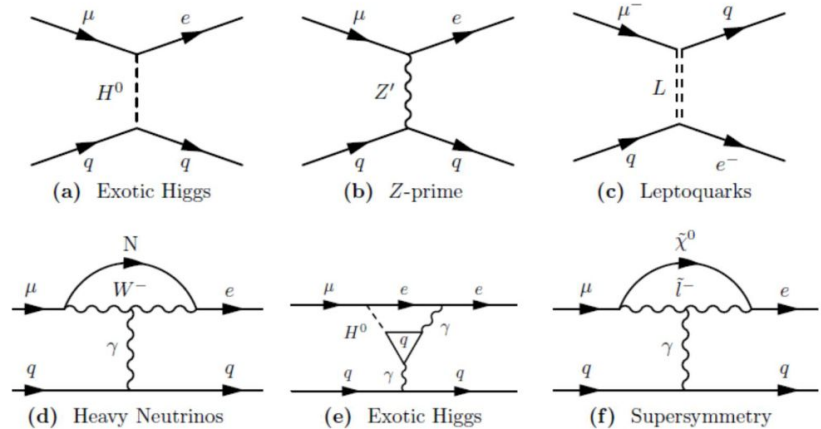
CLFV physics

Neutrino Flavor Violation is observed !



charged Lepton Flavor Violation !? (cLFV)

CLFV Widely predicted in NP models



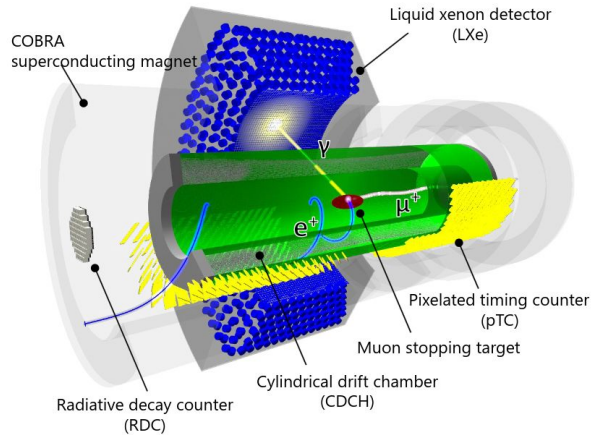
[ref1](#) [ref2](#)

CLFV searches

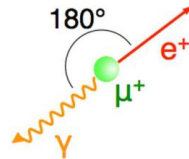
Searching with different channels (tau, mu related) can give us a better understanding of the characteristics of new physics

MEG: Search for $\mu^+ \rightarrow e^+ \gamma$

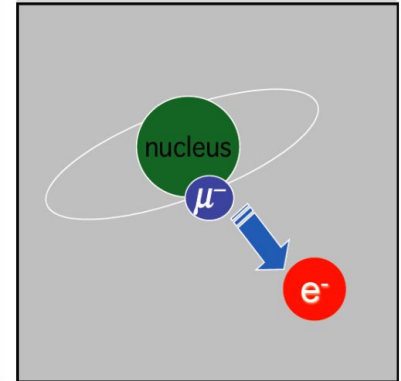
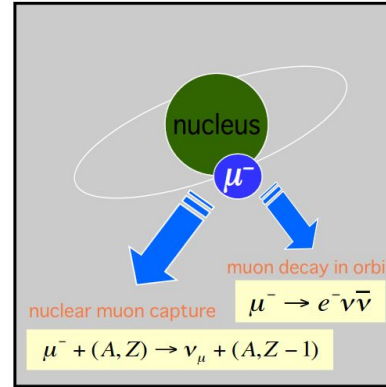
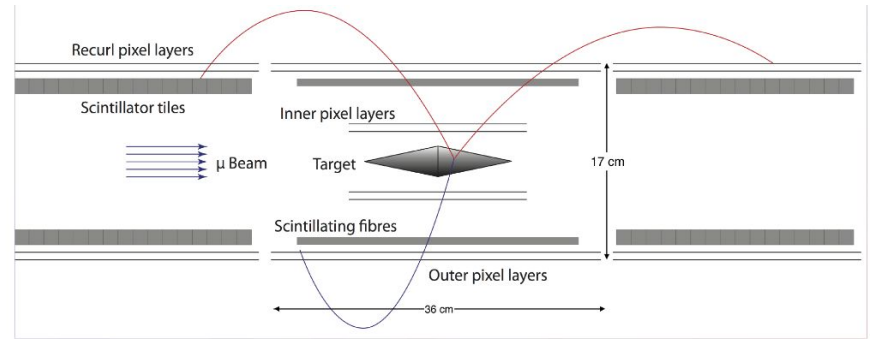
MEG, MEG-II (PSI)



Eur. Phys. J. C (2013) 73:2365

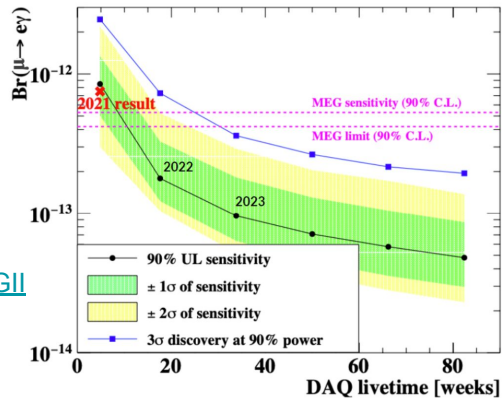
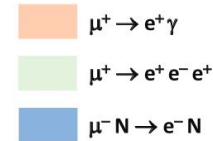
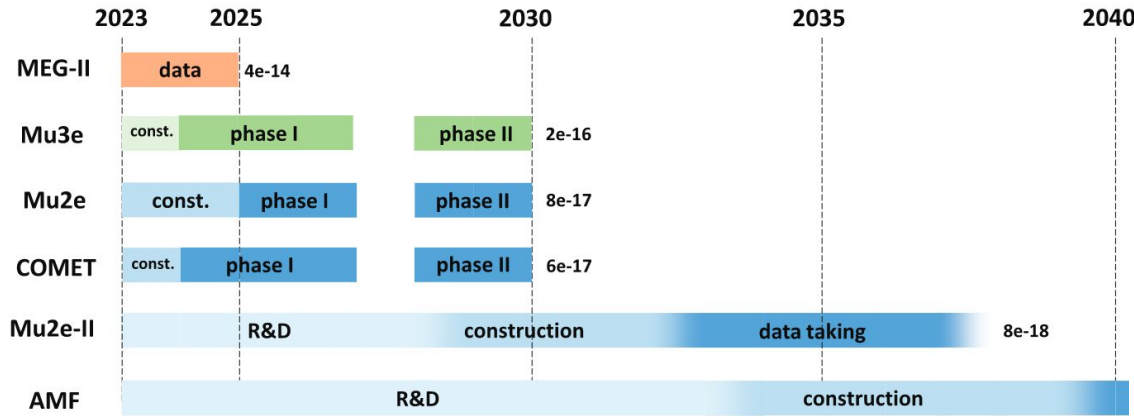


$\mu \rightarrow eee$: Mu3e Experiment



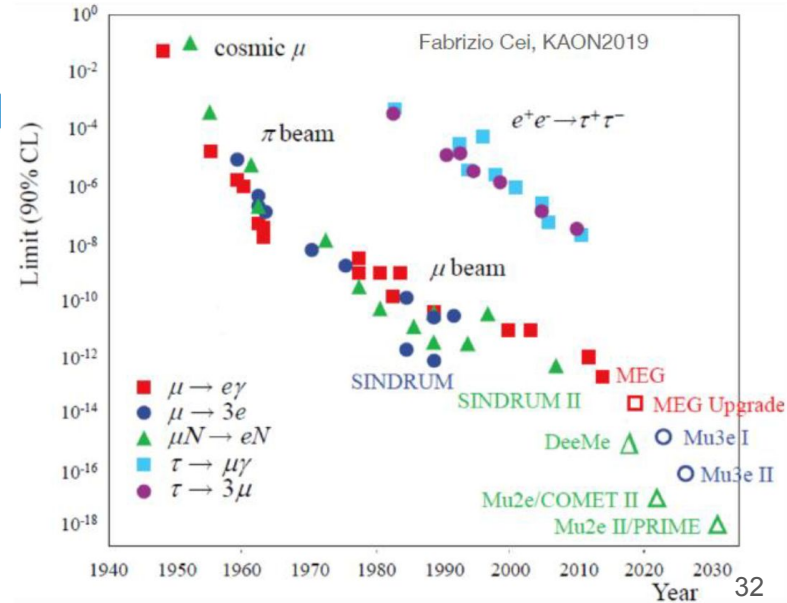
Muon \rightarrow Electron Conversion

CLFV searches



MEGII

- 2024 run in preparation
- 3 more years (including 2024) to reach the goal of 6×10^{-14}
- 3σ discovery if the BR is above $\sim 2 \times 10^{-13}$
- [Remarks]
 - PSI long shutdown in 2027-2028
 - Mu3e Phase I



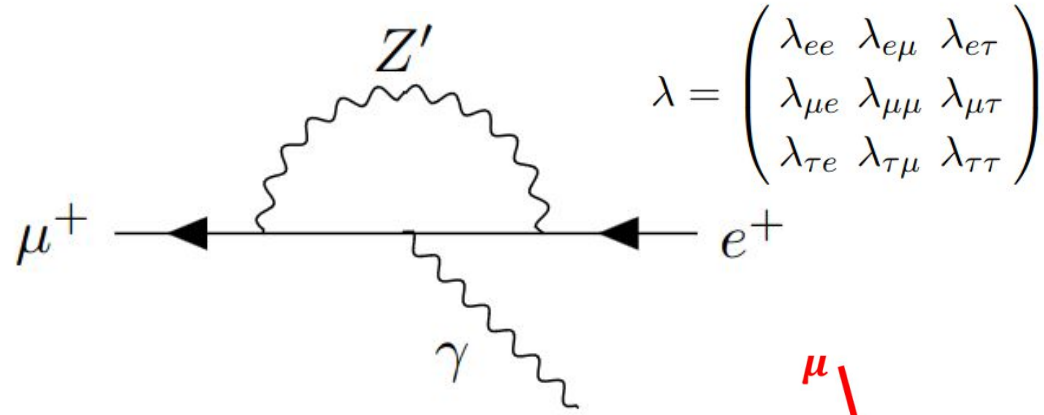
A new yet economic CLFV experiment?

- $\mu \rightarrow e \gamma$

- $\mu \rightarrow e e e$

- $\mu + A \rightarrow e + A$

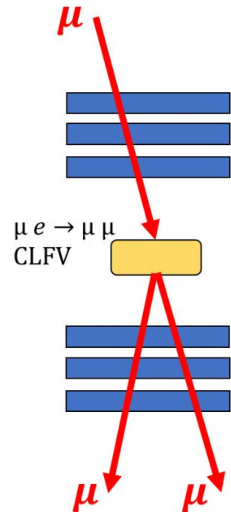
In CLFV
Z' model



$$\lambda = \begin{pmatrix} \lambda_{ee} & \lambda_{e\mu} & \lambda_{e\tau} \\ \lambda_{\mu e} & \lambda_{\mu\mu} & \lambda_{\mu\tau} \\ \lambda_{\tau e} & \lambda_{\tau\mu} & \lambda_{\tau\tau} \end{pmatrix}$$

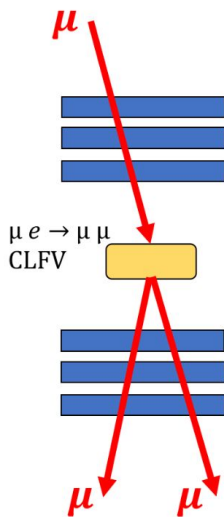
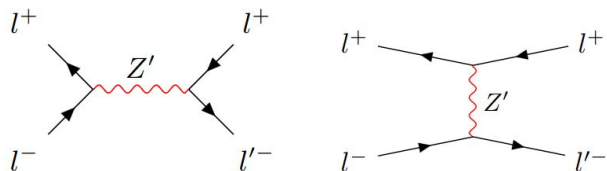
$$\Gamma(\mu \rightarrow e \gamma) = \frac{\alpha G_F^2 m_\mu^3 M_Z^4 (\sin^2 \theta_W (\sin^2 \theta_W - 1/2))^2}{4\pi^4 M_{Z'}^4} (\lambda_{ee} \lambda_{e\mu} m_e + \lambda_{e\mu} \lambda_{\mu\mu} m_\mu + \lambda_{e\tau} \lambda_{\tau\mu} m_\tau + \dots)^2;$$

- There might be more terms, with large cancellation
- No exp on $\mu \rightarrow e \mu \mu$; No exclusive limit on $\lambda_{e\mu} \lambda_{\mu\mu}$



Muon-Electron Threshold Scan

Muon-electron collider CLFV



Muon-on-target muon-electron scattering

Process	$M_{Z'}$ / GeV	E_{μ} / GeV	E_e / MeV	E_{cm} / GeV
$\mu^+e^- \rightarrow e^+e^-$	0.11	0.93	0.511	0.1101
	0.15	11.1	0.511	0.1501
	0.20	28.2	0.511	0.1996
$\mu^+e^- \rightarrow \mu^+\mu^-$	0.22	33.6	0.511	0.2200
	0.25	50.2	0.511	0.2499
	0.30	77.2	0.511	0.2998

- $\mu^+ e^- \rightarrow Z' \rightarrow e^+ e^-$, $\mu^+ \mu^-$ Charged Lepton Flavor Violation
- Resonant production Enhancement
- X=16.7 MeV Anomaly
- Connecting e-mu collider and muon beam experiments

specific beam energy
leads to
specific phase space

Muon-Electron Threshold Scan

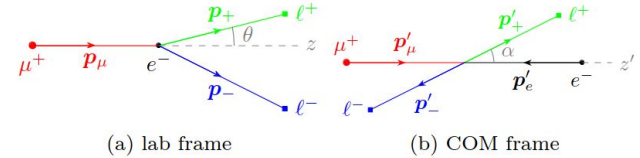
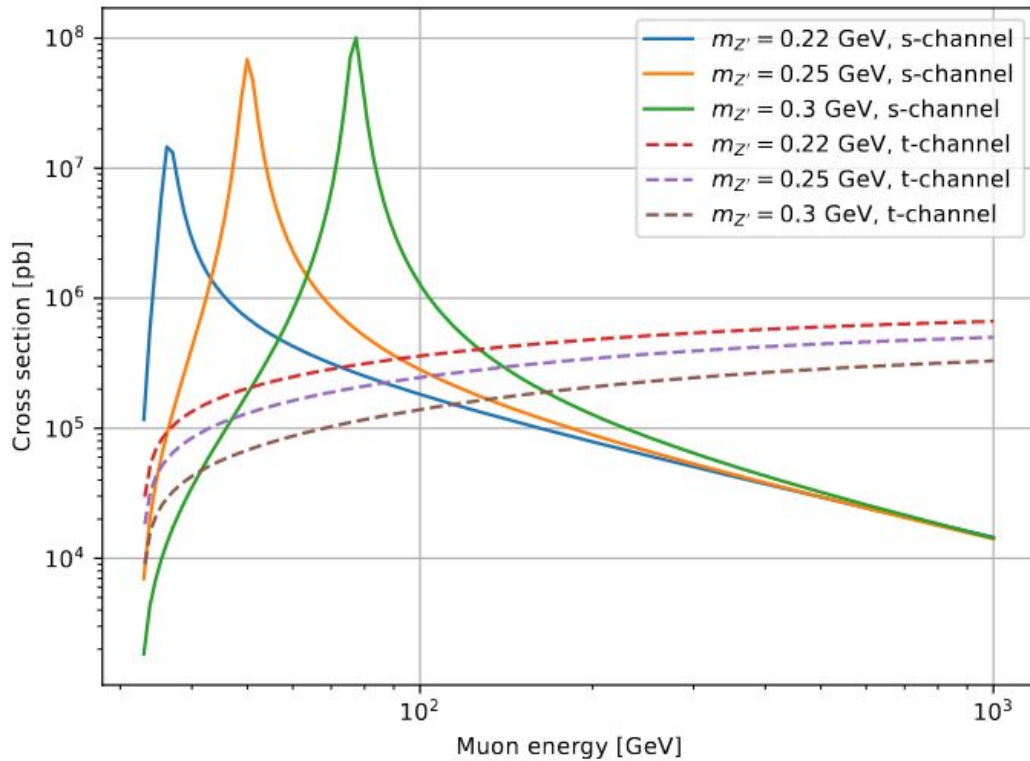
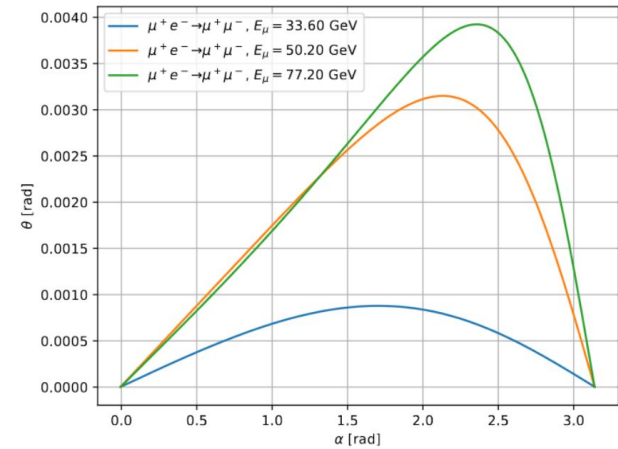


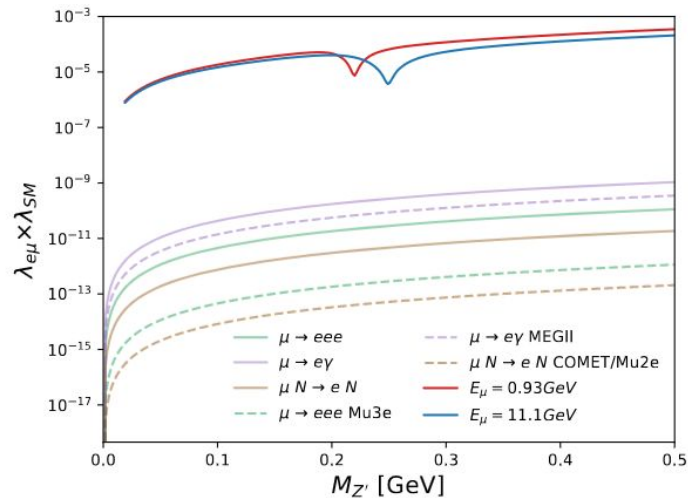
FIG. 4: The $\mu^+e^- \rightarrow \ell^+\ell^-$ process in the (a) lab and (b) COM frames.



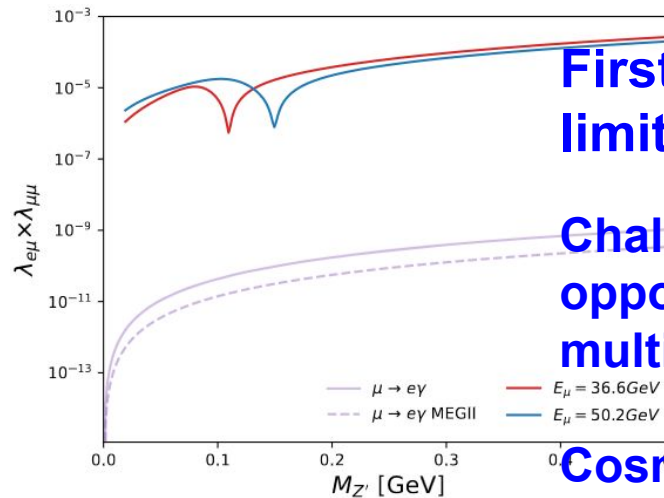
s/t-channel diagrams; on/off-resonance; outgoing angle ~ 0.001 rad 35

Prospected Results by counting

$$R = \frac{dN}{dt} \cdot n \cdot dx \cdot \sigma$$



(a) $\mu^+ e^- \rightarrow e^+ e^-$



(b) $\mu^+ e^- \rightarrow \mu^+ \mu^-$

First ever exclusive limit on $\lambda_{e\mu}\lambda_{\mu\mu}$;

Challenge and opportunity on multi-muon readout

Cosmic Muon or >O(30 GeV) beam

Figure 10: The 90% C.L. upper limit of $\lambda_{e\mu} \times \lambda_{SM}$ (a) and $\lambda_{e\mu} \times \lambda_{\mu\mu}$ (b). The curves are graphed with respect to $M_{Z'}$, representing the limits of the cross section times branching ratio. Additionally, exclusion lines from both present low-energy experiments (shown as solid lines in purple, green and brown) and future experiments (shown as dashed lines in purple, green and brown) are included in the plot.

Geant4 Simulation

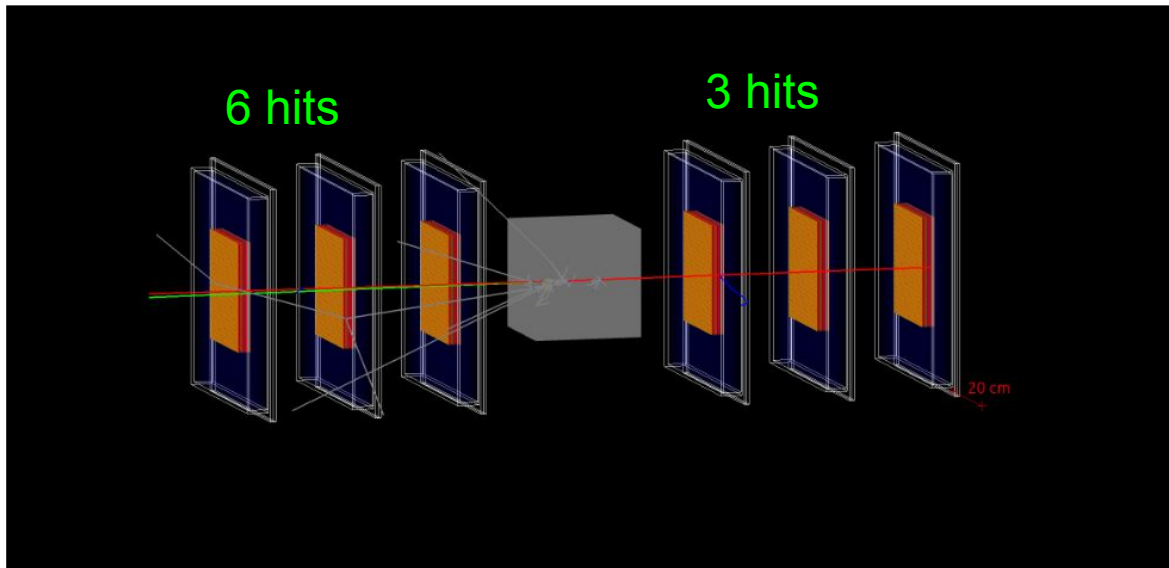


FIG. 6: Geometry configuration and $\mu^+e^- \rightarrow \mu^+\mu^-$ event display of the experiment simulation. Other tracks are shown in gray.

- Muon can lose energy while propagating in material, before hitting with electron
- **A plugin to interface MG with Geant4 efficiently**

Algorithm 1: Efficient $\mu^+e^- \rightarrow \ell^+\ell^-$ event generation

```

function GenerateMuELL( $E_\mu, \vec{p}_\mu, m_\ell$ )
   $E_{\mu 1}, E_{\mu 2}, \sigma_1, \sigma_2, H_1, H_2 \leftarrow \text{AdjacentGridPoints}(E_\mu)$ ;
  if  $E_\mu$  is out of the grid range then
    return no  $\mu^+e^- \rightarrow \ell^+\ell^-$  happens;
  end if
   $w_1 \leftarrow \frac{E_\mu - E_{\mu 2}}{E_{\mu 1} - E_{\mu 2}}, w_2 \leftarrow \frac{E_{\mu 1} - E_\mu}{E_{\mu 1} - E_{\mu 2}}$ ;
   $\sigma \leftarrow w_1\sigma_1 + w_2\sigma_2$ ; // cross section
  if  $\text{Random}(0, 1) < w_1$  then
     $\alpha \leftarrow H_1.\text{Sample}()$ ;
  else
     $\alpha \leftarrow H_2.\text{Sample}()$ ;
  end if // equivalent to  $\alpha \leftarrow (w_1H_1 + w_2H_2).\text{Sample}()$ 
   $\phi \leftarrow \text{Random}(0, 2\pi)$ ;
   $E', p', \gamma, \beta \leftarrow \text{Kinematics}(E_\mu, m_\ell)$ ; // see Appendix A
   $p_{x+} \leftarrow p' \sin \alpha \cos \phi, p_{y+} \leftarrow p' \sin \alpha \sin \phi$ ;
   $p_{z+} \leftarrow \gamma(p' \cos \alpha + \beta E'/2)$ ;
   $\vec{p}_+ \leftarrow \text{ThreeVector}(p_{x+}, p_{y+}, p_{z+})$ ; // see Fig. 3a
   $\vec{p}_- \leftarrow \vec{p}_+.\text{RotateZAxisTo}(\hat{p}_\mu)$ ;
   $\vec{p}_- \leftarrow \vec{p}_- - \vec{p}_+$ ; //  $\hat{z} \leftarrow \hat{p}_\mu$  in Fig. 3a in rotation
  return  $\sigma, \vec{p}_+, \vec{p}_-$ ;
end function

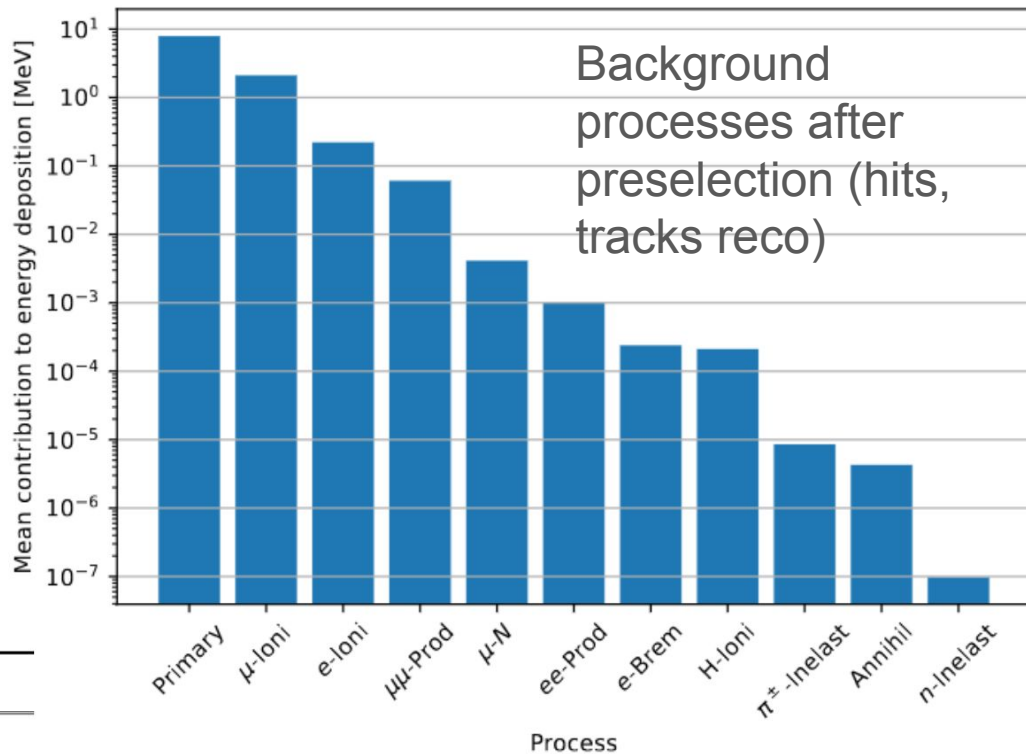
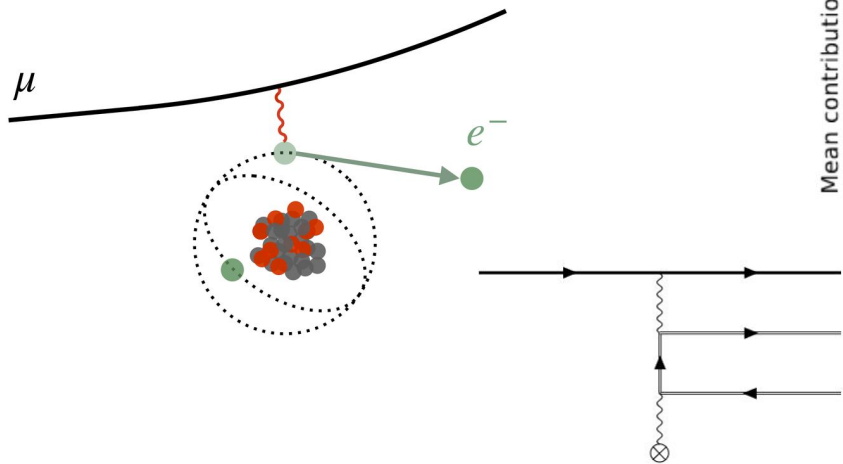
```

Geant4 Simulation

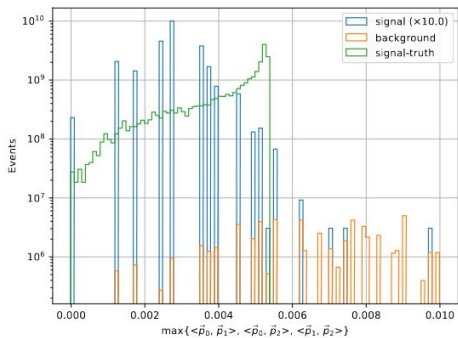
Cluster hits to 3 tracks

$$\chi^2 = \frac{1}{\sigma_t^2} \sum_{t=1}^3 \sum_{h=1}^3 \left(\hat{r}_{th}(\vec{r}_{t1}, \vec{r}_{t3}, z_{th}) - \vec{r}_{th} \right)^2$$

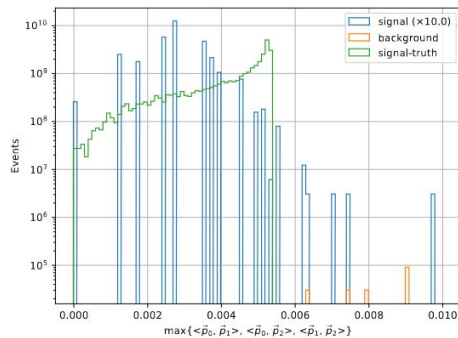
$$= \frac{1}{\sigma_t^2} \sum_{t=1}^3 \left(\hat{r}_{t2}(\vec{r}_{t1}, \vec{r}_{t3}, z_{t2}) - \vec{r}_{t2} \right)^2 \sim \chi^2(6),$$



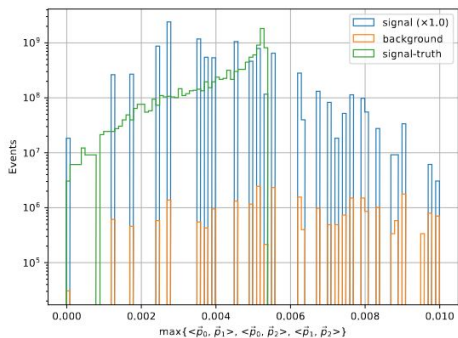
Geant4 Simulation



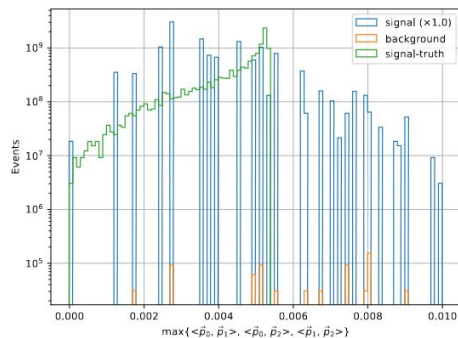
(a) 3 cm Al target



(b) 3 cm Al target, with e -veto



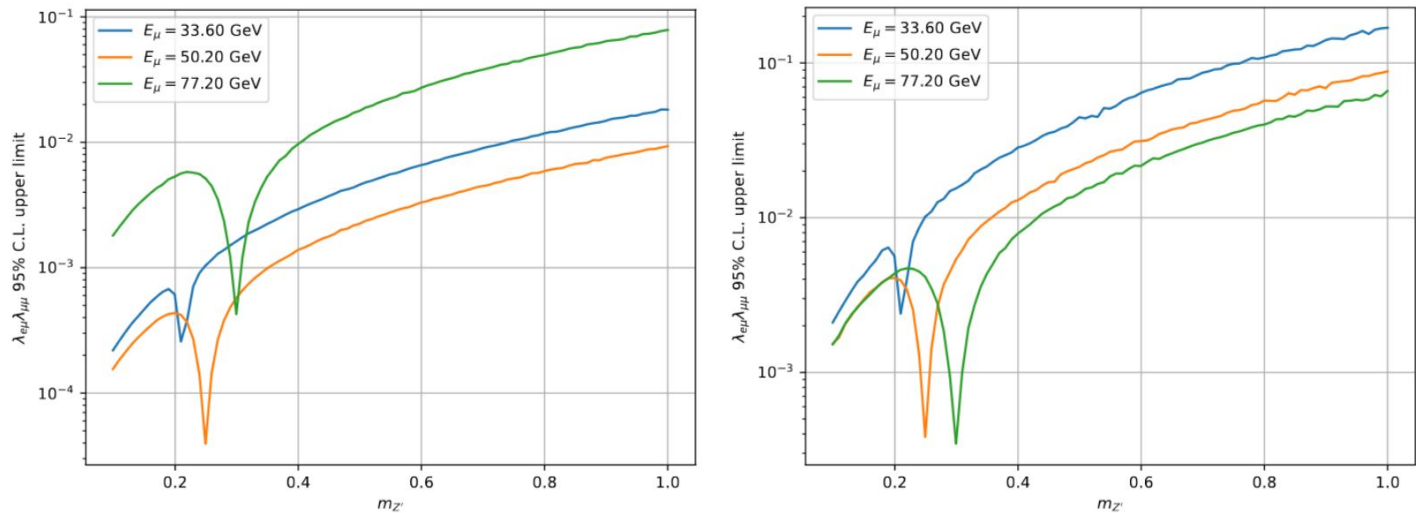
(c) 8 cm Pb target



(d) 8 cm Pb target, with e -veto

FIG. 9: $\max_{i \neq j} \{ \langle \vec{p}_i, \vec{p}_j \rangle \}$ distributions of variant target, where $E_\mu = 50.2$ GeV, $m_{Z'} = 0.25$ GeV, and the $\mu^+e^- \rightarrow \mu^+\mu^-$ process is added with $\lambda_{e\mu}$ scaled to 10 (1) for Al (Pb). The yields are normalized to 3×10^{13} targeting muons corresponding to a one-year accumulation.

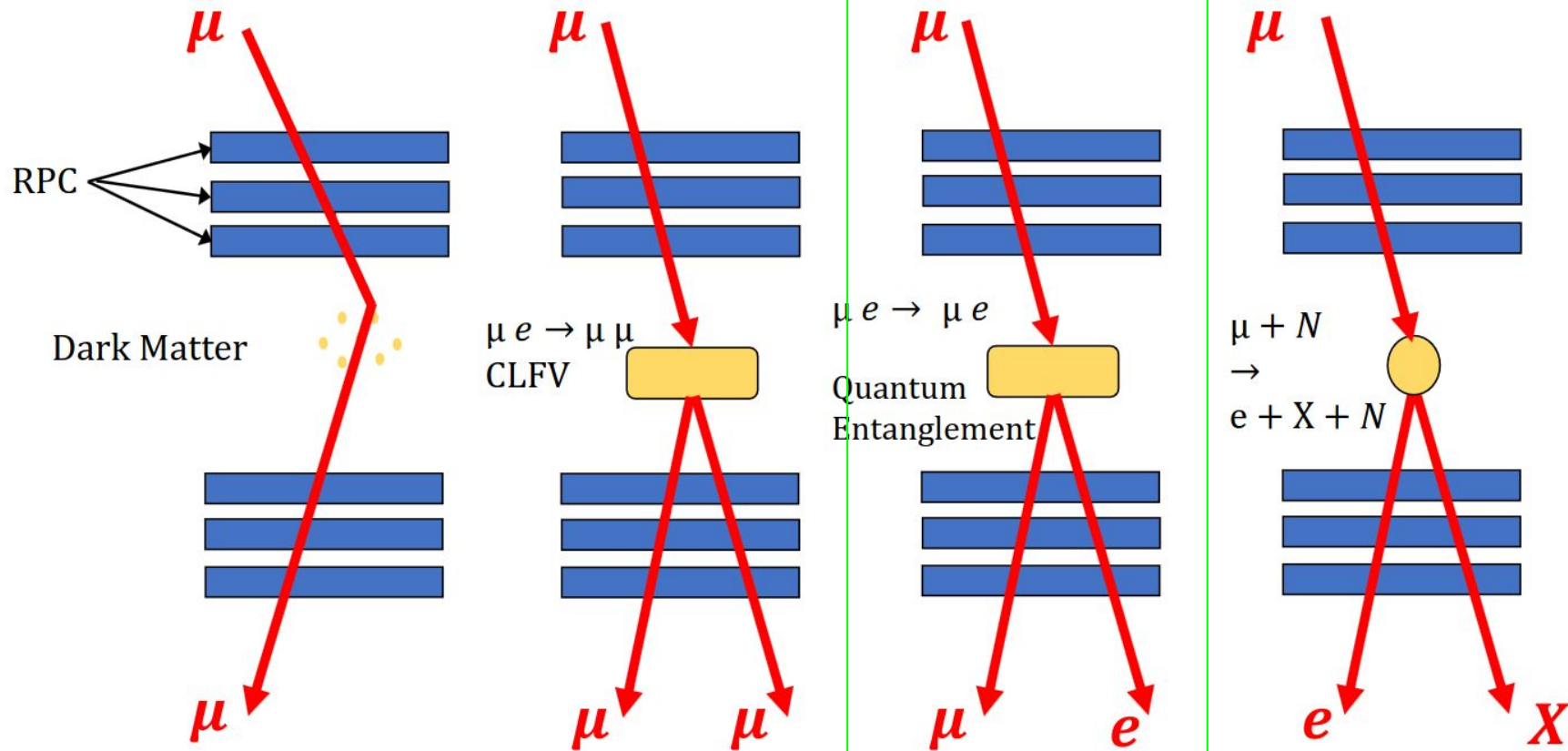
Geant4 Simulation



(a) 3 cm Al target, with e -veto (b) 8 cm Pb target, with e -veto

FIG. 10: 95% C.L. upper limit results of variant target. The yields are normalized to 3×10^{13} targeting muons corresponding to a one-year accumulation.

Probing and Knocking with Muons



Muon Electron Scattering

- [MuonE](#) exploits 160 GeV Muon beam to measure muon electron scattering, and a precise determination of the leading hadronic contribution to the muon $g-2$.
- **Muon electron scattering at lower energy (\sim GeV)** may be interesting to SM test itself, and **Quantum entanglement probe** [PRD 107, 116007 \(2023\)](#):

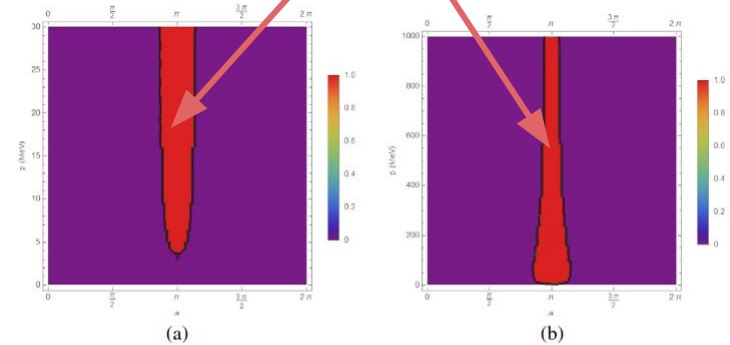
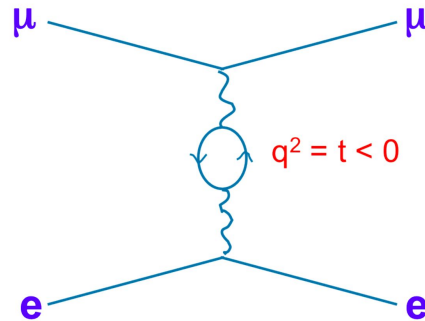
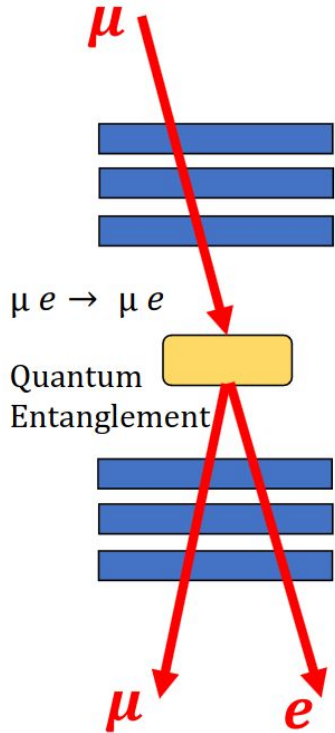
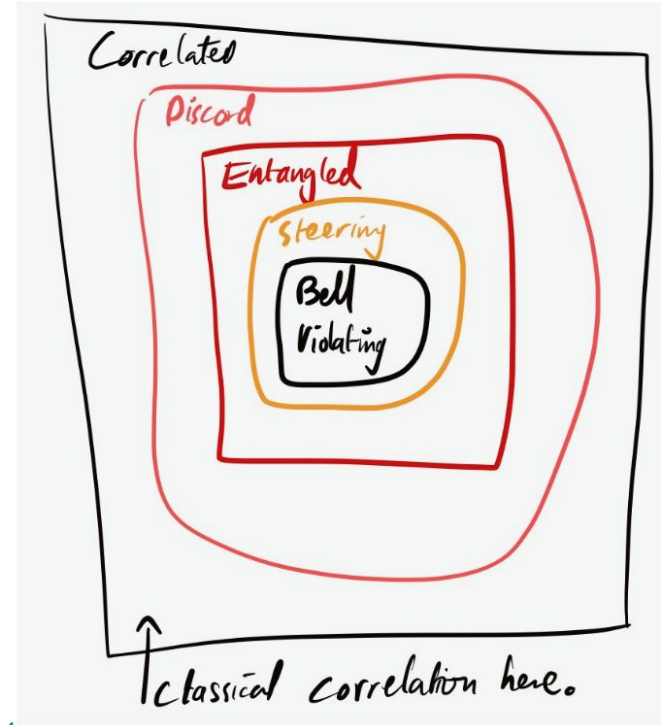
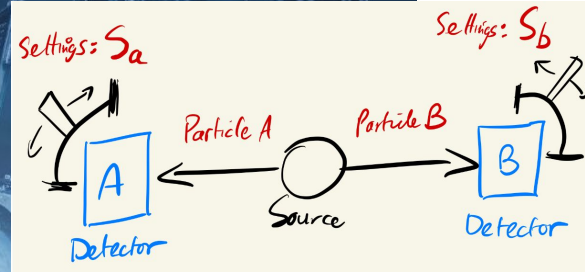
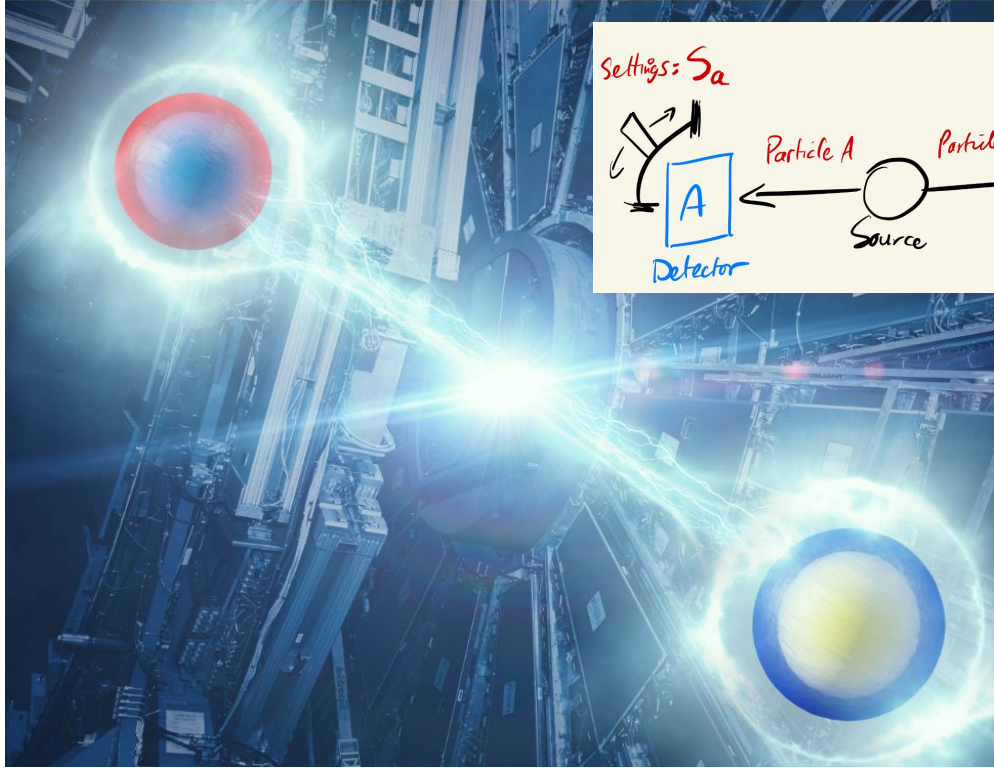


FIG. 15. The red regions correspond to the values of p and θ for which the final state is entangled at low— < 30 MeV—(a) and high— < 1 GeV—(b) energies.

LHC experiments at CERN observe quantum entanglement at the highest energy yet



SUSY2024

Quantum Tomography @ Colliders with or without decays

Tao Han

Pitt PACC, University of Pittsburgh

ATLAS, Oct. 15, 2024



TH, M. Low, A. Wu, arXiv:2310.17696;
K. Cheng, TH, M. Low, arXiv: 2311.09166; 2407.01672; **2410.08303**

2022 Nobel Prize for physics: "pioneering quantum information science"



Clauser Zeilinger Aspect



EPR :



Go! QM Go!

QFT: most precise theory in science!

Our goals:

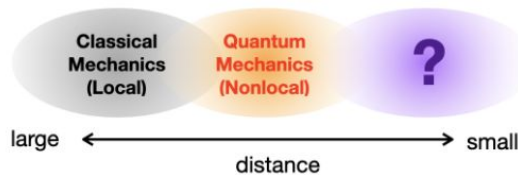
In the framework of QFT, in the HE regime at colliders,

- We lay out the QM predictions / information.
- We calculate the QM correlations / entanglement
- Hope to establish the quantum tomography.
- Understand quantum nature & seek for BSM effects.

High Energy Test of QM

- At very short-distances (high-energies), QM might be modified.

- sense of locality may change (again)
- QM might be modified to be married with gravity



- How can we falsify/test QM?

$$\langle \mathcal{B} \rangle = (\langle AB \rangle + \langle A'B \rangle) + (\langle AB' \rangle - \langle A'B' \rangle)$$

$$\Rightarrow \begin{cases} \langle \mathcal{B} \rangle_{\text{LR}} \leq 2 & \text{Local-Real [CHSH 1969]} \\ \langle \mathcal{B} \rangle_{\text{QM}} \leq 2\sqrt{2} & \text{QM [Tsirelson 1987]} \end{cases}$$



→ High-energy test of Bell inequality is important for testing QM, (rather than testing HLVTs).

- Possible modification of QM?

- No-signalling theories: $\langle \mathcal{B} \rangle_{\text{NS}} \leq 4$ [Cirel'son (1980), Popescu, Rohrlich (1994)]
- Non-linear extensions of QM: [Weinberg (1989), Polchinski (1991), D.E.Kaplan, S.Rajendran, (2021)]

$$i\partial_t |\chi\rangle = \int d^3x \left[\hat{\mathcal{H}}(x) + \langle \chi | \hat{\mathcal{O}}_1(x) | \chi \rangle \hat{\mathcal{O}}_2(x) \right] |\chi\rangle$$

non-linear state-dependent term

Flavor Patterns of Fundamental Particles from Quantum Entanglement?

Jesse Thaler* and Sokratis Trifinopoulos†

Center for Theoretical Physics, Massachusetts Institute of Technology, Cambridge, MA 02139, USA

The Cabibbo–Kobayashi–Maskawa (CKM) matrix, which controls flavor mixing between the three generations of quark fermions, is a key input to the Standard Model of particle physics. In this paper, we identify a surprising connection between quantum entanglement and the degree of quark mixing. Focusing on a specific limit of $2 \rightarrow 2$ quark scattering mediated by electroweak bosons, we find that the quantum entanglement generated by scattering is minimized when the CKM matrix is almost (but not exactly) diagonal, in qualitative agreement with observation. With the discovery of neutrino masses and mixings, additional angles are needed to parametrize the Pontecorvo–Maki–Nakagawa–Sakata (PMNS) matrix in the lepton sector. Applying the same logic, we find that quantum entanglement is minimized when the PMNS matrix features two large angles and a smaller one, again in qualitative agreement with observation, plus a hint for suppressed CP violation. We speculate on the (unlikely but tantalizing) possibility that minimization of quantum entanglement might be a fundamental principle that determines particle physics input parameters.

Muon Electron Scattering for QE

- Lab Frame (electron at rest)

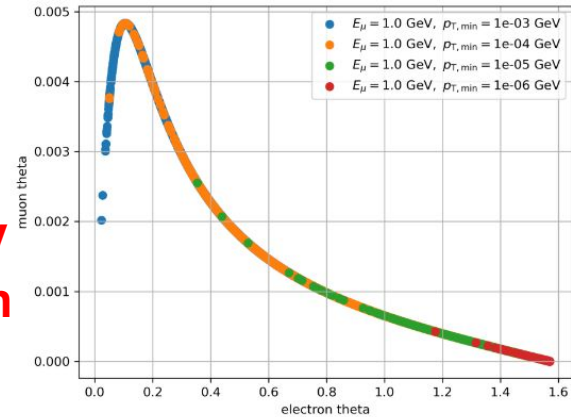
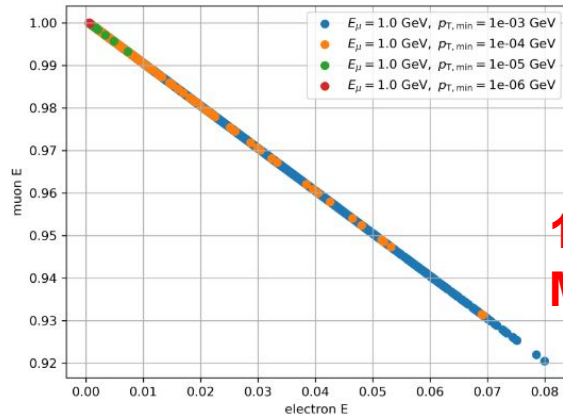
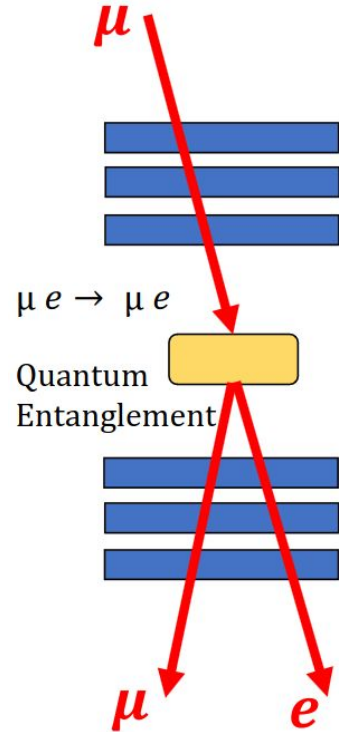
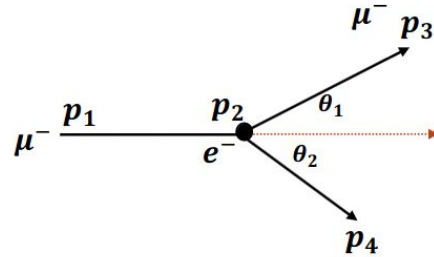
$$p_1 = (E_1, 0, 0, |\mathbf{p}_1|) \quad p_3 = (E_3, |\mathbf{p}_3|\sin\theta_1, 0, |\mathbf{p}_3|\cos\theta_1)$$

$$p_2 = (m_e, 0, 0, 0) \quad p_4 = (E_4, |\mathbf{p}_4|\sin\theta_2, 0, |\mathbf{p}_4|\cos\theta_2)$$

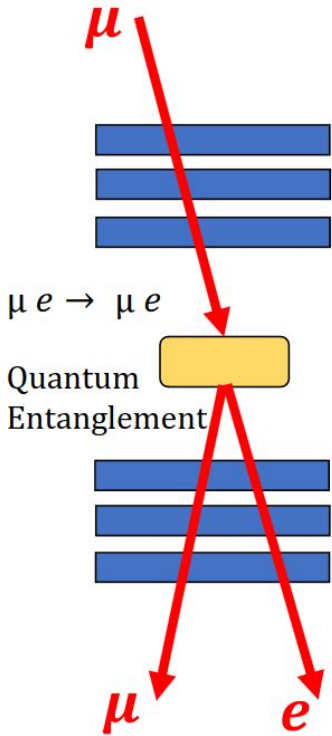
Energy – Momentum relation & Energy conservation:

$$\mathbf{p} = \sqrt{E^2 - m^2}$$

$$E_1 + m_e = E_3 + E_4$$



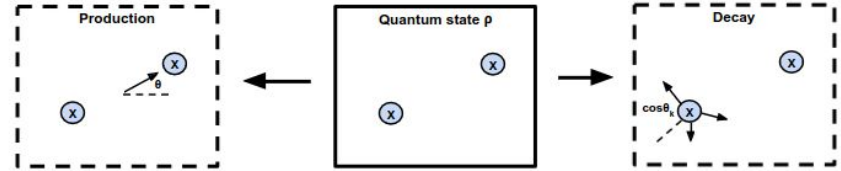
Muon Electron Scattering for QE



$$\mathcal{M}_{(\lambda_1, \lambda_2, \lambda_3, \lambda_4)}(p_1, p_2, p_3, p_4) \longrightarrow \mathcal{M}_{(\lambda_1, \lambda_2, \lambda_3, \lambda_4)}(\theta_\mu, \theta_e, E_3)$$

$$\rho = \frac{\mathcal{M}_{\lambda_3, \lambda_4} \mathcal{M}_{\bar{\lambda}_3 \bar{\lambda}_4}^*}{\sum_{\text{spins}} |\mathcal{M}|^2}$$

$$\mathcal{M}_{\lambda_3, \lambda_4} = \frac{1}{4} \sum_{\lambda_1, \lambda_2} \mathcal{M}(\lambda_1, \lambda_2, \lambda_3, \lambda_4)$$



Quantum Tomography at Colliders: With or Without Decays

Kun Cheng,^{1,*} Tao Han,^{1,†} and Matthew Low^{1,‡}

¹PITT PACC, Department of Physics and Astronomy,
University of Pittsburgh, 3941 O'Hara St., Pittsburgh, PA 15260, USA

(Dated: October 14, 2024)

The interpretation of groups of particle spins at colliders as quantum states has opened up the possibility of using colliders for quantum information. While most efforts have focused on utilizing the decays of the particles to infer their spins to reconstruct the quantum density matrix, we show that the production kinematics of the particles provides sufficient information about the spins to establish quantum tomography without using the decays. We perform a comparative study, highlighting the advantages and disadvantages of using this “kinematic approach” relative to the usual “decay approach.” Since the kinematic approach leverages the simplicity of scattering kinematics, this approach promises to achieve the optimal statistical results for quantum tomography at colliders.

PITT-PACC-2408

<https://arxiv.org/abs/2410.08303>

QE criterion [ref](#) [ref2](#)

- 量子纠缠发生的条件: **Peres-Horodecki criterion**: 如果共有系统(joint state) 的密度矩阵的偏转置(partial transpose)有一个非正的本征值, 则量子态中存在纠缠。

$$\rho = \begin{pmatrix} A_{11} & A_{12} & \dots & A_{1n} \\ A_{21} & A_{22} & & \\ \vdots & & \ddots & \\ A_{n1} & & & A_{nn} \end{pmatrix} \xrightarrow{\text{偏转置}} \rho^{TB} = \begin{pmatrix} A_{11}^T & A_{12}^T & \dots & A_{1n}^T \\ A_{21}^T & A_{22}^T & & \\ \vdots & & \ddots & \\ A_{n1}^T & & & A_{nn}^T \end{pmatrix}$$

- 因此 ρ^{TB} 最起码必须一个本征值是负的
- Negativity is useful : $N = \sum_i \frac{(|\lambda_i| - \lambda_i)}{2}$
- N = 0: no entanglement
- N > 0 : entanglement present!

2024/11/10

HEP phenomenology: PDF, FMC, SMFit

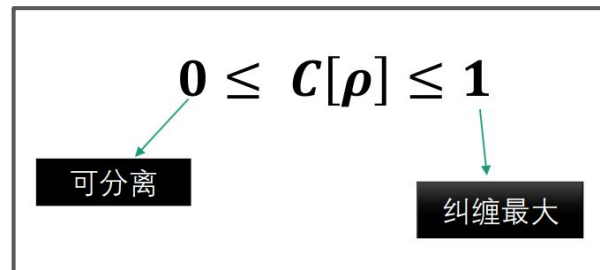
- 量子纠缠大小: concurrence $C[\rho]$

$$\tilde{\rho} = (\sigma_y \otimes \sigma_y) \rho^* (\sigma_y \otimes \sigma_y)$$

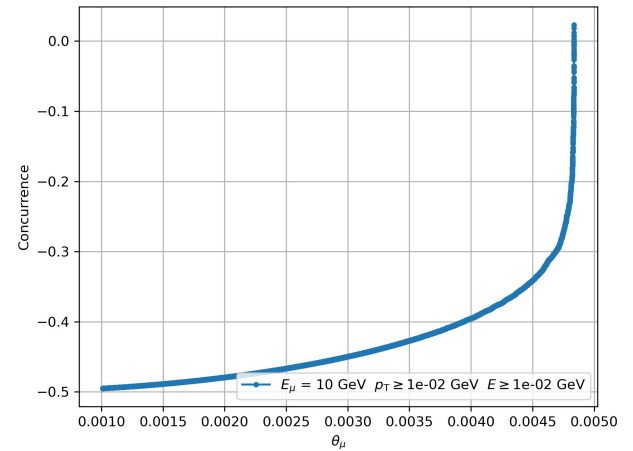
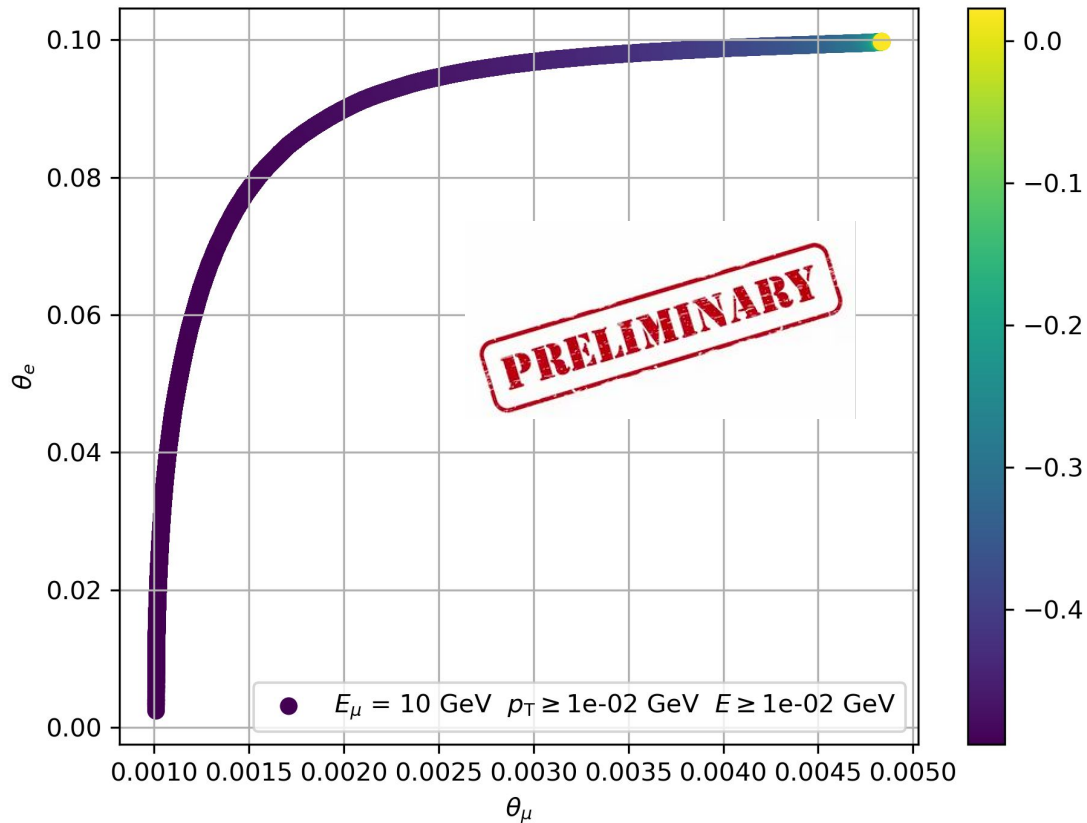
$$R = \sqrt{\sqrt{\rho} \tilde{\rho} \sqrt{\rho}}$$

$$C(\rho) \equiv \max(0, \lambda_1 - \lambda_2 - \lambda_3 - \lambda_4)$$

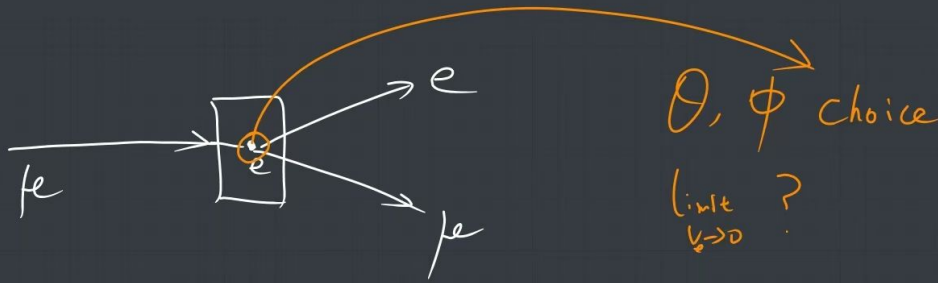
λ_i 是 R 矩阵的本征值且: $\lambda_1 > \lambda_2 > \lambda_3 > \lambda_4$



Simulated QE results



Simulated QE results



θ, ϕ choice

limit
 $v \rightarrow 0$?

$$\gamma = \frac{1}{\sqrt{1 - (v/c)^2}}$$

$$\gamma = E/m_0$$

Only muon: can provide QE test over vast range

0.5 GeV

1 GeV

10 GeV

0.3 GeV

$\gamma \approx 5$

$\gamma \approx 10$

$\gamma \approx 100$

$\gamma \approx 3$

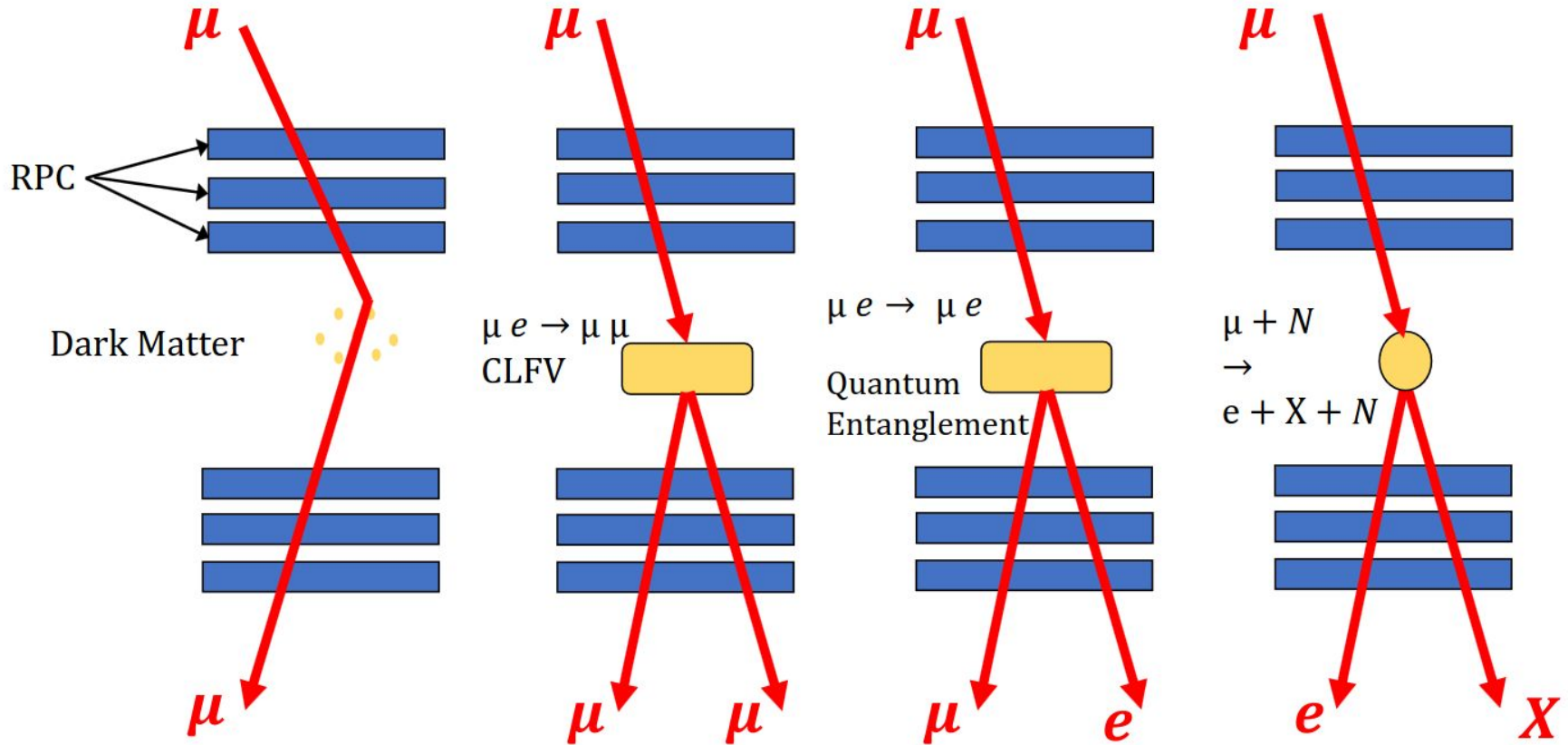
$v \approx 0.98c$

$v = 0.995c$

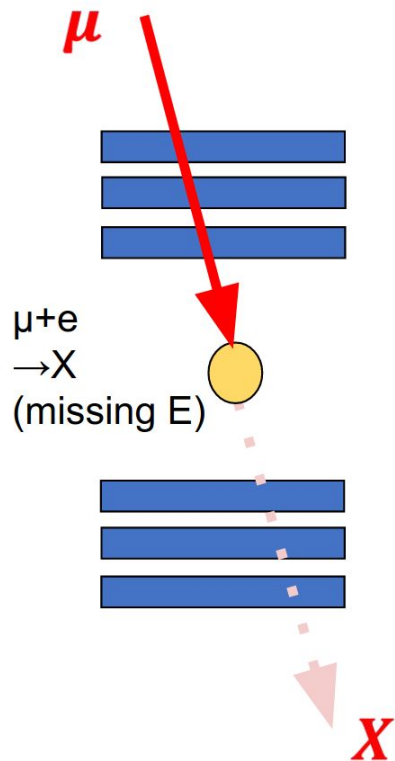
$v = 0.99995c$

$v = 0.942c$

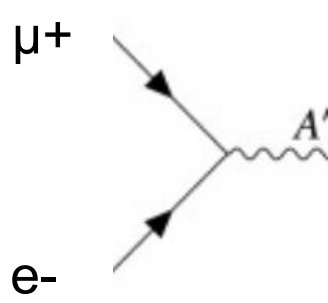
Probing and Knocking with Muons



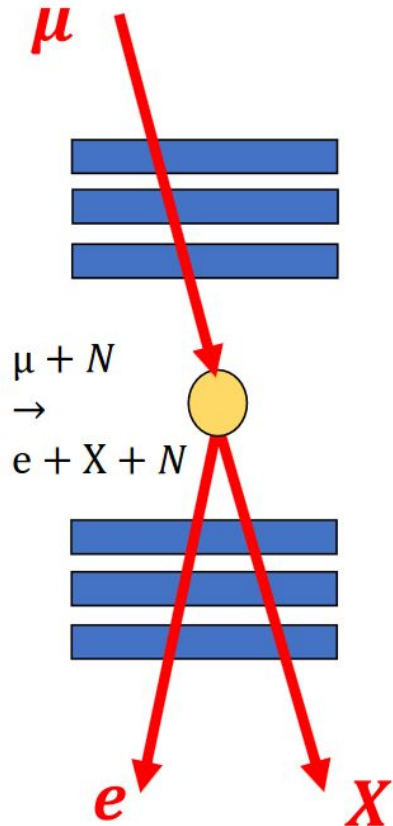
Flavor Changing Dark X



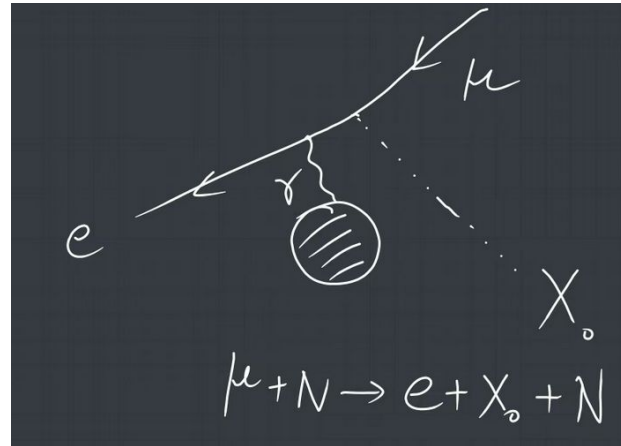
- Muon electron ($\mu^+ e^-$) annihilation into missing energy signal
- Similar proposal (ERC supported [POKER](#)) for e^+e^- annihilation
 - [Phys. Rev. D 88 \(2013\), 114015](#)
 - [Phys.Rev.D 104 \(2021\) 9, L091701](#)
 - [Exp results](#) with NA64
- Muon beam energy can be lowered down
 - If X mass is small enough
- Can be interpreted as $\text{Br}(\mu^- \rightarrow e + X)$ for low mass X
 - and compared with [TWIST](#)
- To be implemented within G4
 - Our own implementation
 - Or using [DMG4](#)



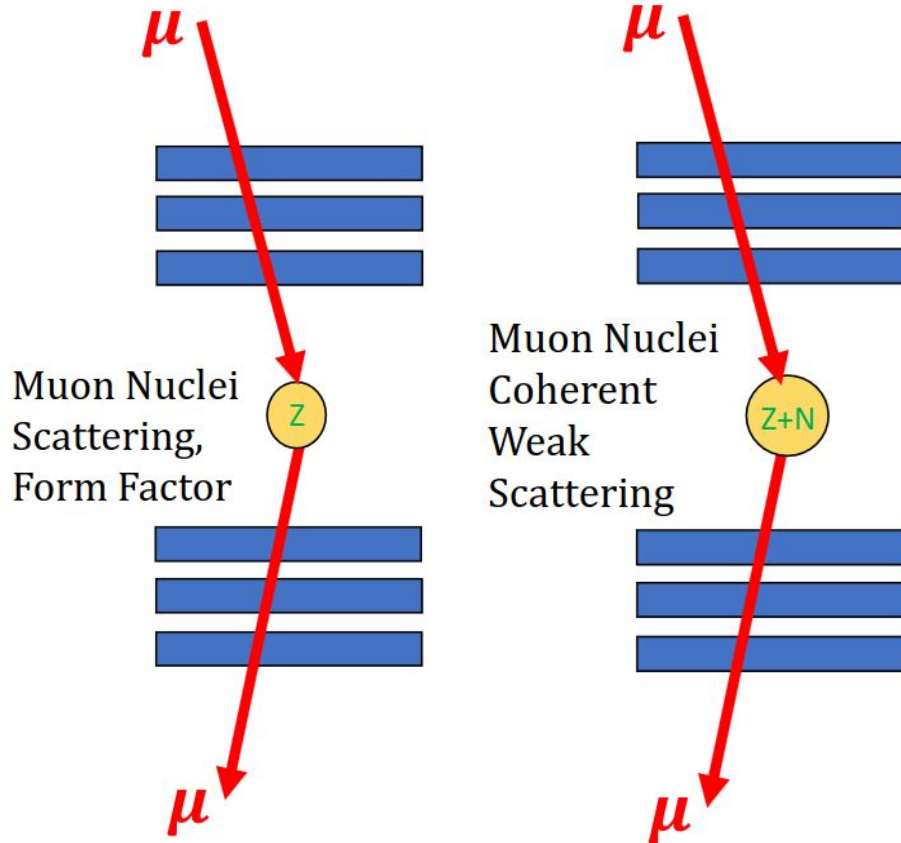
Muon's two body 'decay'



- Lepton family number violation by searching for $\mu \rightarrow e X_0$
- Previous limit from the Twist Collaboration: [Phys. Rev. D 91, 052020 \(2015\)](#)
- We are aiming at muon on target searches (**works also for X_0 heavier than muon**).
 - Require Calorimeter to veto backgrounds
 - Can also be put under flavor changing Dark Matter



Muon nuclei scattering



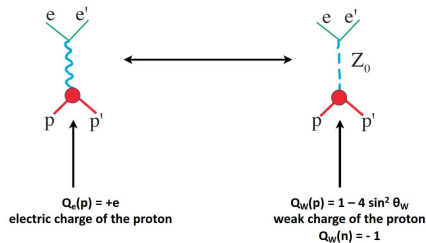
- Various scattering experiment to measure nuclei structure
 - [JLAB](#) 12-24 GeV electron scattering
 - CERN [COMPASS](#) and [AMBER](#) muon project
- **With 0.1-1 GeV Muon beam, we may measure independently**
 - Nuclei (charge) form factor
 - Coherent Weak scattering
 - ...

Muon nuclei scattering for weak mixing angle and neutron skin?



The role of the weak mixing angle

The relative strength between the weak and electromagnetic interaction is determined by the **weak mixing angle**: $\sin^2(\theta_w)$



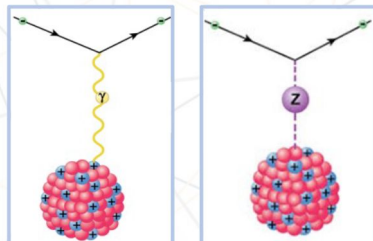
$\sin^2 \theta_w$: a **central parameter** of the standard model accessible through the weak charge



PVES

Parity Violating Electron Scattering: powerful tool to measure both the nuclear weak charge and the weak nuclear radius

Polarized electrons that scatter off a nucleus: both **electromagnetic** and **weak interaction**



Interaction mediated by the photon and so mostly sensitive to the charge (proton) distribution

Interaction mediated by the Z boson and so mostly sensitive to the weak (neutron) distribution.

QWeak

Polarized electrons \rightarrow build an asymmetry

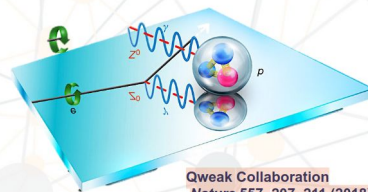
$$\mathcal{A}_{pv} = \frac{\sigma_+ - \sigma_-}{\sigma_+ + \sigma_-} \approx - \frac{G_F Q^2}{4\pi\alpha\sqrt{2}} \frac{Q_W F_W(Q^2)}{Z F_{ch}(Q^2)}$$

Nuclear Weak Charge

Weak distribution

Charge distribution

Charge distribution is well known from electromagnetic scattering



Qweak Collaboration
Nature 557, 207–211 (2018)



This formula is in PWBA, Coulomb distortion effect must be taken into account

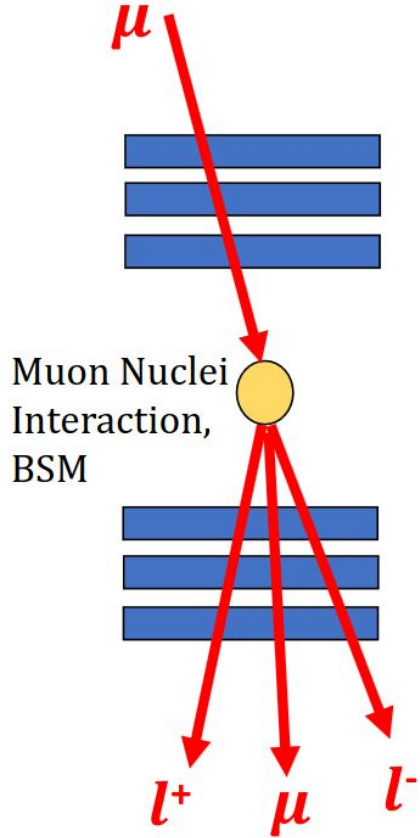
Measure Flux of Scattered electrons:

- no pile-up (double count losses)
- sensitive to small electr. fields.
- no separation of phys. process

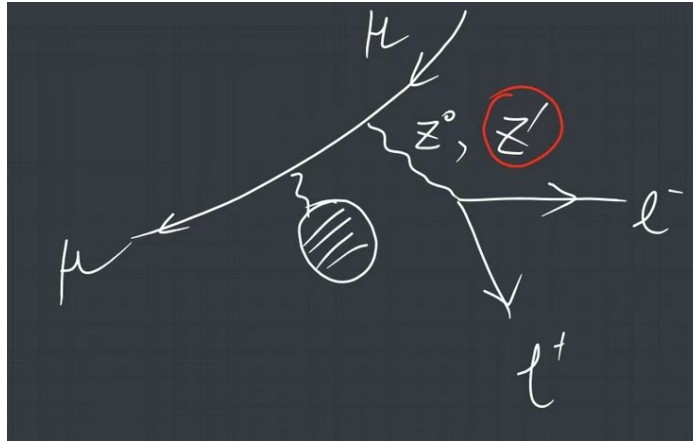
However, need polarized muon beams?
These electron beam energy ~ 1 GeV

Low energy muon may give new ways (coherent) to probe weak distribution?

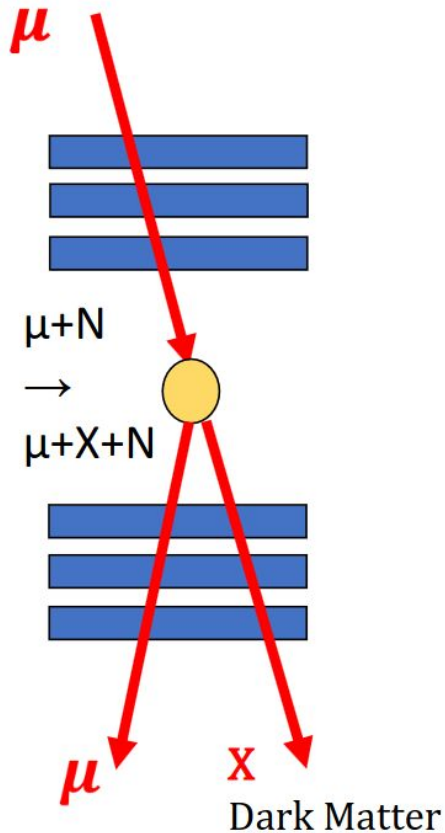
Muon nuclei scattering



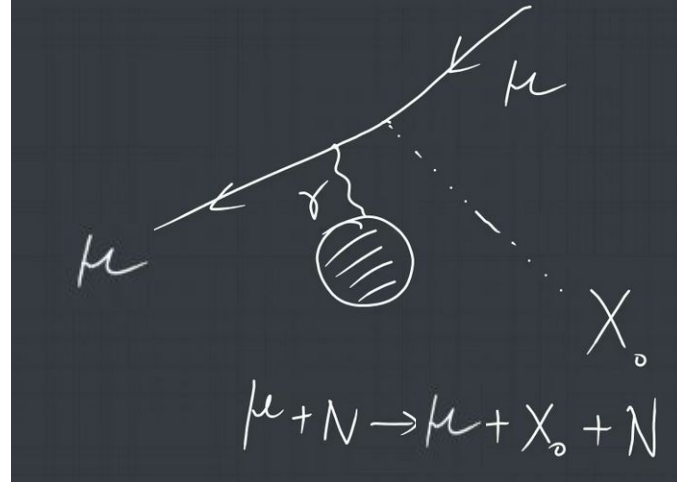
- Rare Muon Nuclei scattering processes to be measured and explored.
- Verify Geant4 Simulation [Tool](#)
- **Sensitive to various BSM, including**
 - **the Zprime CLFV,**
 - **or DM decays into visible signals**



Dark Matter from Muon nuclei scattering



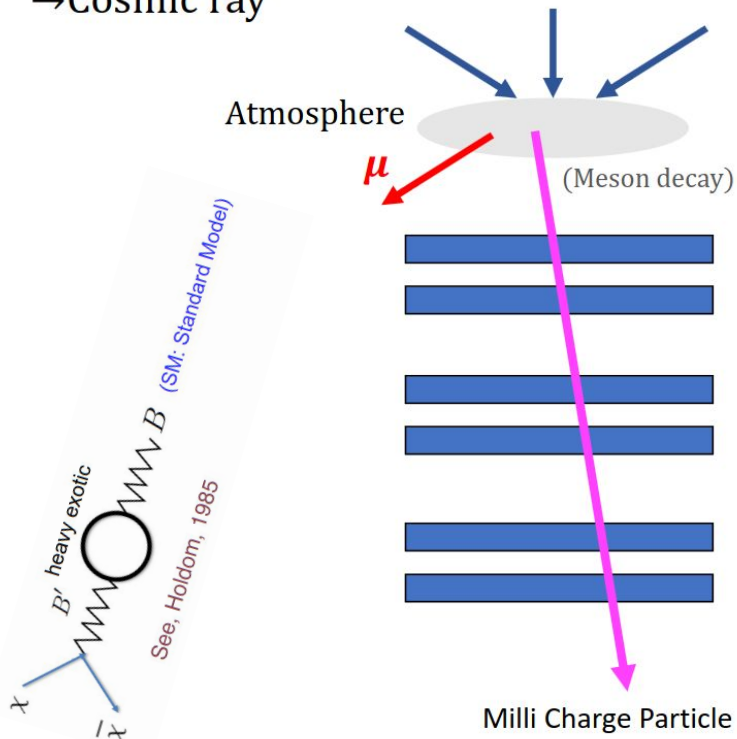
- Exploration of the Muon $g-2$ and Light Dark Matter explanations in [NA64](#) with the CERN SPS high energy muon beam
- Our limit may be weak than NA64mu.
- Can still be used to verify Geant4 Simulation Tool



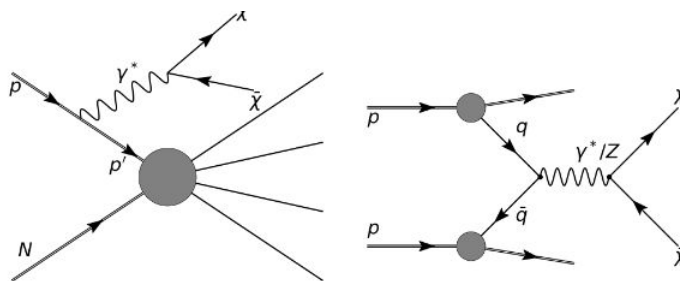
Milli-Charged Particle Searches

Telescope

→ Cosmic ray



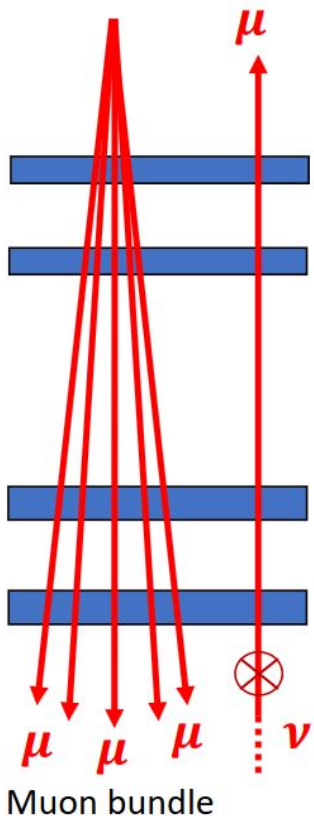
- Heavy millicharged particles may be produced from the atmosphere when high energy cosmic rays collide with nuclei
 - Theoretical predictions [here](#)
- **Can be detected at PKMu detectors**
 - **PID and optimization to be done.**



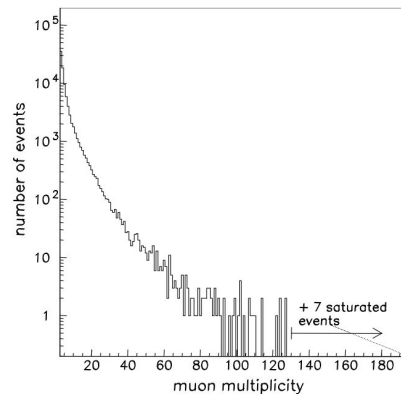
Also from meson decay

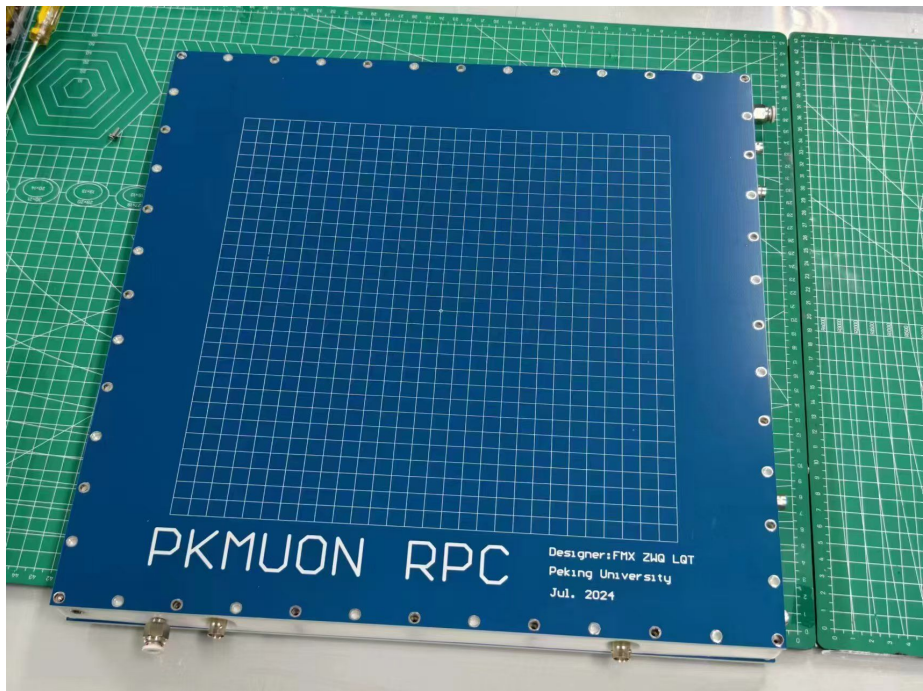
FIG. 2. Feynman diagrams for MCP production through proton bremsstrahlung (left) and the Drell-Yan process (right).

Muon Bundle from Cosmic Ray

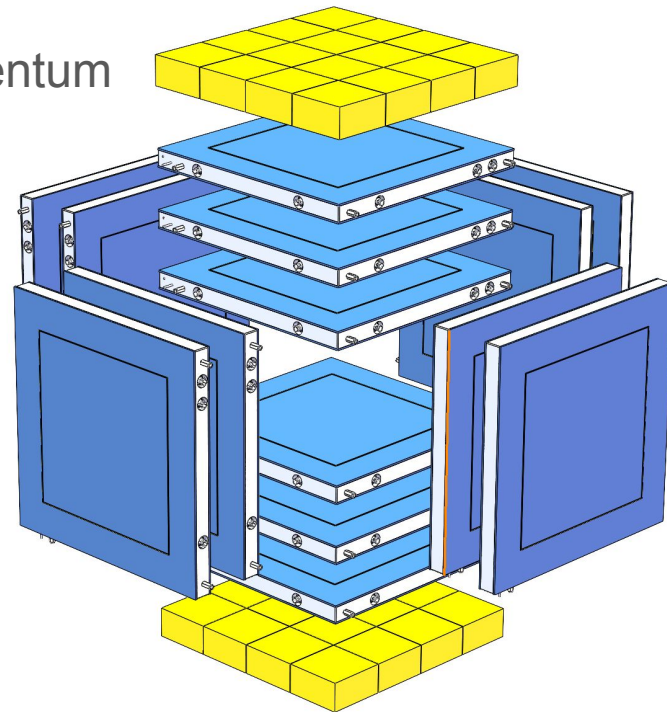


- Multi-muon bundles in cosmic ray showers detected, e.g., with the [DELPHI](#) detector at LEP
 - Could be sensitive to heavy ion elements in CR
- With large area PKMu detectors, it is possible to detector muon bundles and trace back to the origin points in the atmosphere ($\sim O(10)$ km)
- Again, challenges and opportunities to read out multi-muons!





PID;
Momentum



Melody, CIADS, HIAF Muon beams

Melody: approved and the first Chinese Muon beam will be built in 5 years.

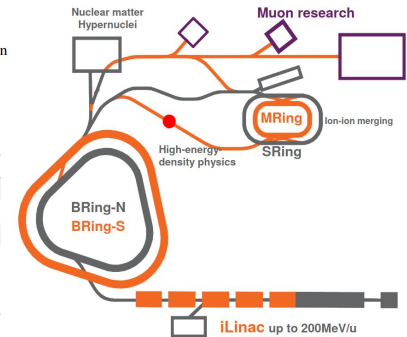
	Surface Muon	Negative Muon	Decay Muon
Proton Power (kW)	20	Up to 100	Up to 100
Pulse width (ns)	130 to 10	500	130 to 10
Muon intensity (/s)	$10^5 \sim 10^6$	Up to 5×10^6	Up to 5×10^6
Polarization (%)	>95	>95	50~95
Positron (%)	<1%	NA	<1%
Repetition (Hz)	1	Up to 5	Up to 5
Terminals	2	1~2	2
Muon Momentum (MeV/c)	30	30	Up to 120
Full Beam Spot (mm)	10 ~ 30	10 ~ 30	10~30

HIAF & HIAF-U



- **BRing-N**: 34Tm, 569m, 3Hz
- **SRing**: 17(25)Tm, 270.5m, accumulation/compression
- **BRing-S**: 86Tm, 3Hz, superconducting
- **MRing**: 45Tm, superconducting, beam merging

	Particle (GeV/u)	Intensity (ppp)	Est. time
FAIR	2.7	$^{238}\text{U}^{28+}$ 5×10^{11}	2025
NICA	4.5	$^{197}\text{Au}^{32+}$ 4×10^9	2022
FNAL	8.0	p 6.8×10^{13}	2028
	3.0	$^{238}\text{U}^{35+}$ 2×10^{12}	
HIAF-U	9.1	$^{238}\text{U}^{92+}$ 1×10^{12}	2032
	25	p 4×10^{14}	



~30 MeV, ~100 MeV,

~1GeV

PoCA

- The point of closest approach (PoCA) algorithm
- The angular scattering distribution is approximately Gaussian

$$\sigma_{\theta} = \frac{13.6 \text{ MeV}}{\beta c p} \sqrt{\frac{L}{L_0}} \left[1 + 0.038 \ln \frac{L}{L_{\text{rad}}} \right] \approx \frac{13.6}{p} \sqrt{\frac{L}{L_0}}$$

❖ p : momentum, βc : velocity, L : depth of the material, L_{rad} : radiation length of the material

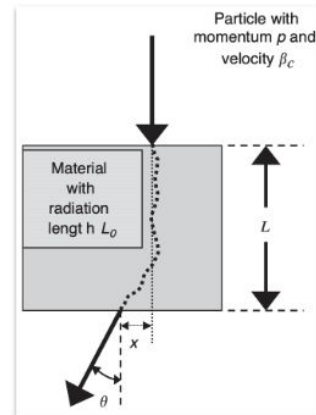
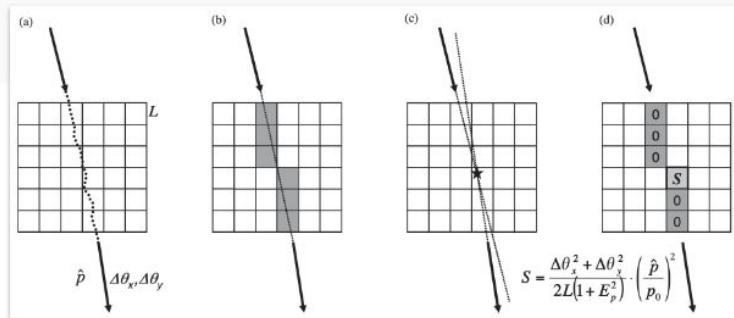
- Scattering strength: establish a nominal muon momentum (3 GeV, for example), and define the mean square scattering of nominal muons per unit depth of a material

$$\lambda_{\text{mat}} = \left(\frac{13.6}{p_0} \right)^2 \frac{1}{L_{\text{rad}}} \approx \sigma_{\theta_0, \text{mat}}^2$$

❖ depends only on material radiation length, and varies strongly with material Z

- Multiple muons income and scatter with material, and we measure it in two orthogonal planes x and y . If we know the path length L_i and the momentum p_i of each muon through the material:

$$\hat{\lambda} = \frac{1}{N} \sum_{i=1} N \left(\frac{p_i^2}{p_0^2} \cdot \frac{\theta_{xi}^2 + \theta_{yi}^2}{2L_i} \right)$$

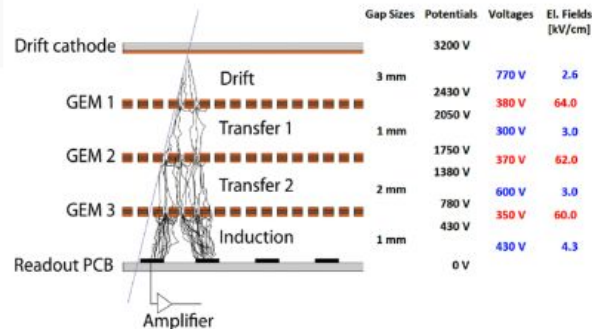


GEM

→ Triple-GEM detector installed in the CMS experiment

- ❖ Improve trigger capabilities and muon measurements
- ❖ Excellent performance: rate $> 10 \text{ kHz/cm}^2$, time resolution $\sim 8 \text{ ns}$, spatial resolution $\sim 200 \mu\text{m}$

CMS TDR

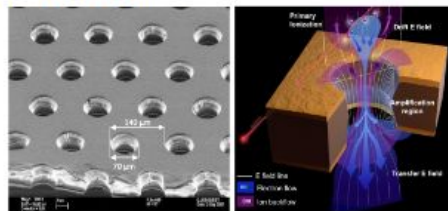


Schematic view of a triple-GEM detector

→ Electron amplification structure and flexible readout structures

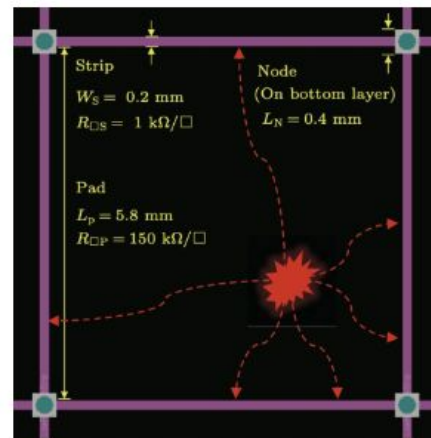
→ Pixel readout VS resistive anode readout method

- ❖ Challenge: Large amount of small pixels
- ❖ Good comparable spatial resolution but less electronic channels



→ Design our exclusive readout for the specific requirements of PKU-Muon GEM detectors.

- ❖ Hit position reconstruction algorithm ongoing



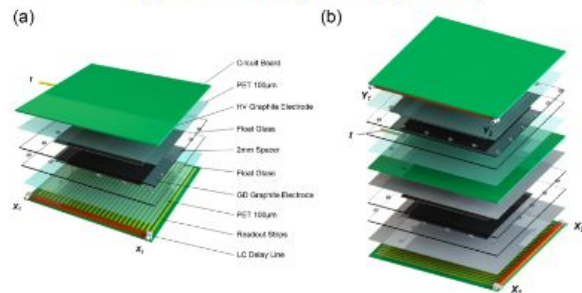
Structure diagram of the basic resistive anode cell

RPC

Compact Muon Solenoid



(a) Prototype glass RPC
(b) One RPC with two structure get X and Y signals respectively



→ RPC — R. Santonico (in 1980s)

- ❖ simple and robust structure, long-term stability, good timing resolution, easy-maintenance and low cost

→ PKU RPC R&D History

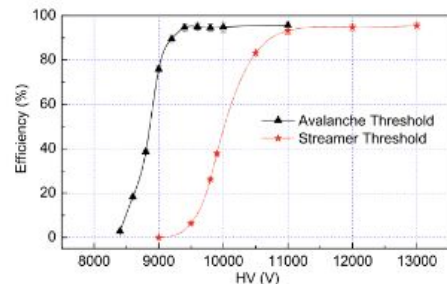
- ❖ **CMS Muon Trigger RPCs**, assembled and tested by PKU (2002)
- ❖ Combination of glass RPC & Decay-line Readout ([Qite Li et. al.](#))

→ Glass RPC MT Prototype in 2012

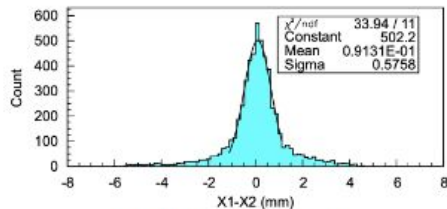
- ❖ Effective area of the electrode: $20 \times 20 \text{ cm}^2$
- ❖ Readout electronics: decay-line, charge-division methods

→ Good and stable performance so far!

- ❖ Positional resolution: $\sim 0.5 \text{ mm}$, detection efficiency: $> 90\%$



Efficiency curves for the glass RPC



Distribution of X1-X2